III-1 Pretreatment Effect Research - Characterization Studies with 100 Fe/0.3 Cu/0.8 K Catalyst

III-1.1 Experimental

III-1.1.1 Catalyst Preparation Procedure

A 100 Fe/0.3 Cu/0.8 K in parts by weight catalyst was used for this study. The catalyst preparation involved two steps: preparation of the Fe-Cu precursor followed by potassium impregnation. The constant pH precipitation technique was used to prepare the Fe-Cu catalyst precursor. This technique has been described in detail elsewhere (Bukur et. al. 1989a,b). In brief, the catalyst precursor was continuously precipitated at 82 ^{o}C from a flowing aqueous solution containing Fe and Cu nitrates at the desired Fe/Cu ratio, using aqueous ammonia. The precipitate was then thoroughly washed by distilled water by vacuum filtration. After a vacuum drying step, the potassium promoter was added as aqueous $KHCO_3$ solution via an incipient wetness pore-filling technique. The catalyst was then dried at 120^{o}C for 16 h in a vacuum oven. The dried catalyst was calcined in air at 300^{o}C for 5 h. The powder so obtained was then crushed and sieved to diameter between 0.25 to 0.55 mm (30/60 mesh).

III-1.1.2 Catalyst Characterization Equipment and Procedures

The catalyst composition was verified by Atomic Absorption using a Varian SpectrAA-30 spectrophotometer. Required amount of catalyst was dissolved in 10 ml of concentrated HCl followed by dilution with distilled water to 100 ml. Portions of this sample were then tested for the composition of Cu, K, and Fe. The standard solutions for Cu, Fe, and K were obtained from Aldrich.

Catalysts were pretreated in a SS-316 fixed bed reactor (1/2 inch OD, 4 3/4 inch long). This unit was used only for characterization studies following pretreatment in

different reducing environments. The unit has two valves 2.5 inches from either end of the reactor. At the end of pretreatment, the catalyst was purged with helium and the two valves were closed to isolate the reactor from the remainder of the apparatus. The reactor was then removed without exposing the catalyst to an oxidizing atmosphere. Typically 1.5-2.5 g of catalyst was used in pretreatment studies.

Powder X-ray diffraction patterns of the catalyst samples before pretreatment, after pretreatment, and after FT reaction (used catalysts) were obtained on a Geigerflex (Rigaku, Dmax Series) system using Cu-Kα radiation (λ= 1.54 Å) starting from 2θ=2° to 85° at the rate of 4°/min. For the determination of particle size by line broadening method the region of interest was scanned at a lower scan rate of 0.5°/min. The instrumental line broadening was determined from NBS standard SRM-640 powder sample. The particle size was determined using standard Scherrer's formula with K=0.9 after applying the instrumental line broadening correction.

The BET surface area and the pore size distribution of the catalysts before and after pretreatment were determined by N_2 physiosorption at 77 K using a Micromeritics Digisorb 2600 system. The samples were degassed at 150°C for 12 h prior to each measurement.

Transmission electron micrographs of the catalysts were obtained using a Zeiss transmission electron microscope (Model No.10C). The particle size range was obtained directly from the micrographs by simple observation.

Isothermal reduction experiments with H_2 and CO at atmospheric pressure were carried out in a fixed bed reactor system similar to that used for FT synthesis. The system was equipped with an on-line mass spectrometer (Dycor, M200; Ametek, Inc.) and a gas chromatograph (Carle, AGC Series 400). Prior to reduction by either CO or H_2, the catalyst was heated in a flow of helium from room temperature to 280°C. Reductant gas was admitted in the system through switch from He to either CO or H_2 (space velocity = 3 Nl/g-cat/h). The effluent gases were monitored continuously by

mass spectroscopy. A fast rate of data acquisition (1 minute intervals) for the species of interest was achieved by the use of a computerized data acquisition system. A proper background correction was employed for all the species of interest. Care was taken to heat all the lines and the vacuum chamber in order to avoid condensation of products. The composition of gases was also determined frequently using gas chromatography.

III-1.1.3 Catalyst Handling and Sample Preparation

After each pretreatment procedure, the reactor was sealed (air-tight) in an inert gas atmosphere and then transferred to a glove box. The samples for XRD analyses were removed in an inert atmosphere and then transferred to specially designed sample holders. These sample holders could be sealed in the glove box and then placed directly in the X-ray machine. The sample holders were made out of Plexiglas which does not yield any diffraction peaks. The above procedure prevents exposure of catalyst samples to an oxidizing environment.

The used catalysts were removed from a fixed bed reactor in an inert atmosphere at the end of the reaction tests. The sample handling procedure was similar to that described above. Catalyst samples removed from the top, bottom, and/or middle portions of the reactor were analyzed separately. In addition, for the used catalysts samples from each portion of the reactor, separation from glass beads (used as a diluent during FT synthesis) was necessary. This was achieved by magnetic separation in a glove box. Such a separation was found to increase the intensity of the XRD peaks significantly.

The used catalyst samples from slurry reactor tests were separated from wax in an inert atmosphere. This was carried out in a glove box filled with He as follows: A slurry sample (about 20 g), from the slurry sampling cylinder was dissolved in warm and degassed varsol and then filtered at about 80°C. The filter cake, mostly catalyst and a small amount of wax, was then rinsed with warm degassed toluene. The wet

cake was dried in vacuum at ambient temperature in a pre-chamber of the glove box. After drying, the cake was put into an extraction thimble which was placed inside a small sealable plastic bag. The thimble was then transferred into the Soxhlet extraction apparatus in a glove bag filled with He. The extraction apparatus was then taken out of the glove bag and the extraction is carried out first with xylene for 36 h, followed by methyl ethyl ketone for 18 h. The top of the condenser unit was closed so that no air could enter the system during extraction. At the end of extraction, the catalyst was transferred again to the glove box where it was removed from the thimble and sealed in sample vials and stored or placed in specially designed sample holders for characterization by XRD.

The sample preparation for the BET/PSD analyses was also carried out in an inert atmosphere (in a glove box). The BET sample tubes were loaded with the required amount of catalyst and then sealed in the glove box in order to prevent air oxidation of the catalysts.

The TEM, however, was carried out in air at room temperature. This indeed exposed the samples to an oxidizing environment. However, this is not expected to change the catalyst morphology and particle size drastically. The samples were dispersed on the carbon film sample holder supported by 300 to 400 mesh specimen mounts. The probe was then mounted in the microscope and micrographs at several magnifications were obtained.

III-1.2 Results and Discussion

III-1.2.1 Atomic Absorption

The composition of the catalyst determined by Atomic Absorption Spectroscopy was found to be 100 Fe/ 0.33 Cu/ 0.84 K which is in agreement with the nominal composition of the catalyst.

III-1.2.2 X-Ray Diffraction

As-Prepared and Calcined Catalyst

XRD patterns of the as-prepared and calcined catalysts are shown in Figure III-1.1. XRD pattern exhibited by both samples is typical of Fe_2O_3 (hematite, rhombohedral) phase. The as-prepared catalyst, however, exhibited broader peaks indicating partial crystallinity of the Fe_2O_3 phase (see Figure III-1.1a). On calcination in air at 300°C the crystallinity improved considerably as seen from Figure III-1.1 b. The phases identified are listed in Table III-1.1. The average particle sizes for the as-prepared and the calcined catalyst estimated by X-ray line broadening technique using the corresponding slow scans were 16 and 14 nm respectively, and are listed in Table III-1.1.

Reduced (Pretreated) Catalyst

The XRD patterns of the catalyst obtained after pretreatment with H_2 at different temperatures and flow rates are shown in Figure III-1.2. After pretreatment with H_2 at 220°C for 1h with a flow rate of 3550 cc/min, the bulk Fe_2O_3 phase was reduced to Fe_3O_4 (Figure III-1.2a). Several peaks corresponding to metallic Fe were also detected. The phases identified are listed in Table III-1.1. The particle size of Fe_3O_4 was estimated from the corresponding slow scan and is listed in Table III-1.1. The average particle size increased on reduction with hydrogen from 14 to 19 nm. This suggests that the Fe_2O_3 particles agglomerate on reduction to form Fe_3O_4 (magnetite). It should be noted that this is not merely a result of thermal treatment since the catalyst was already calcined at 300°C.

The XRD pattern obtained after pretreatment with H_2 at 250°C for 2 h with a flow rate of 3550 cc/min is illustrated in Figure III-1.2 b. Peaks corresponding to metallic iron only could be detected indicating that Fe_2O_3 is completely reduced to Fe. The particle size increased significantly after reduction at 250°C (from 14 to 24 nm).

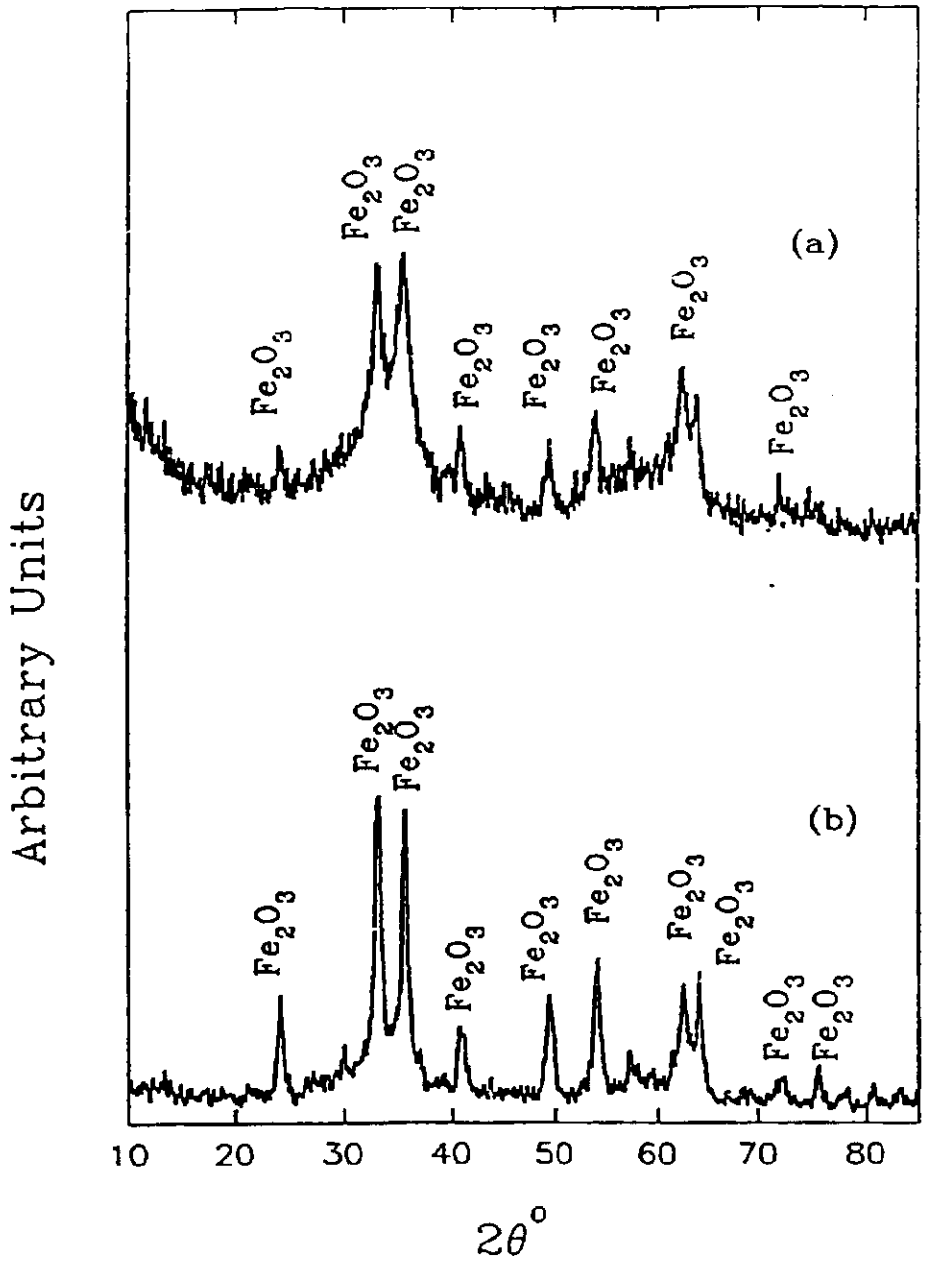

Figure III-1.1 XRD patterns of 100 Fe/0.3 Cu/0.8 K catalyst: a) as prepared; b) calcined in air at 300°C for 5h.

Table III-1.1 Summary of XRD and TEM Results of Pretreated 100 Fe/0.3 Cu/0.8 K Catalyst Samples.

Run No.	Pretreatment Conditions	Phases Detected by XRD[a]	Average Particle Size Determined by XRD (nm)	Particle Size Range Determined by TEM (nm)
C0308-3 (as prep)	None	Fe_2O_3	16	---
C0308-3 (calcined)	Air, 300°C, 5 h	Fe_2O_3	14	26-28
FA-2451	H_2, 220°C, 1h, 3550 cc/min	Fe_3O_4, α-Fe	19 (Fe_3O_4)[b]	12-31
FA-2491	H_2, 250°C, 2h, 3550 cc/min	α-Fe	24	31-64
FA-2751	H_2, 280°C, 8h, 85 cc/min	Fe_3O_4, α-Fe	33 (α-Fe)[b]	35-61
FA-2531	CO, 280°C, 8h, 85 cc/min	χ-Fe_5C_2	*	11-56
FA-2601	H_2/CO=0.67, 280°C, 8h, 85cc/min	χ-Fe_5C_2	*	22-43
FA-2581	H_2/CO=2, 310°C, 6h, 1200 cc/min	χ-Fe_5C_2	*	17-80

a: Phases are in decreasing order of relative intensities.

b: Indicates the phase used for particle size determination.

*: The particle sizes could not be estimated using XRD because of overlapping signals.

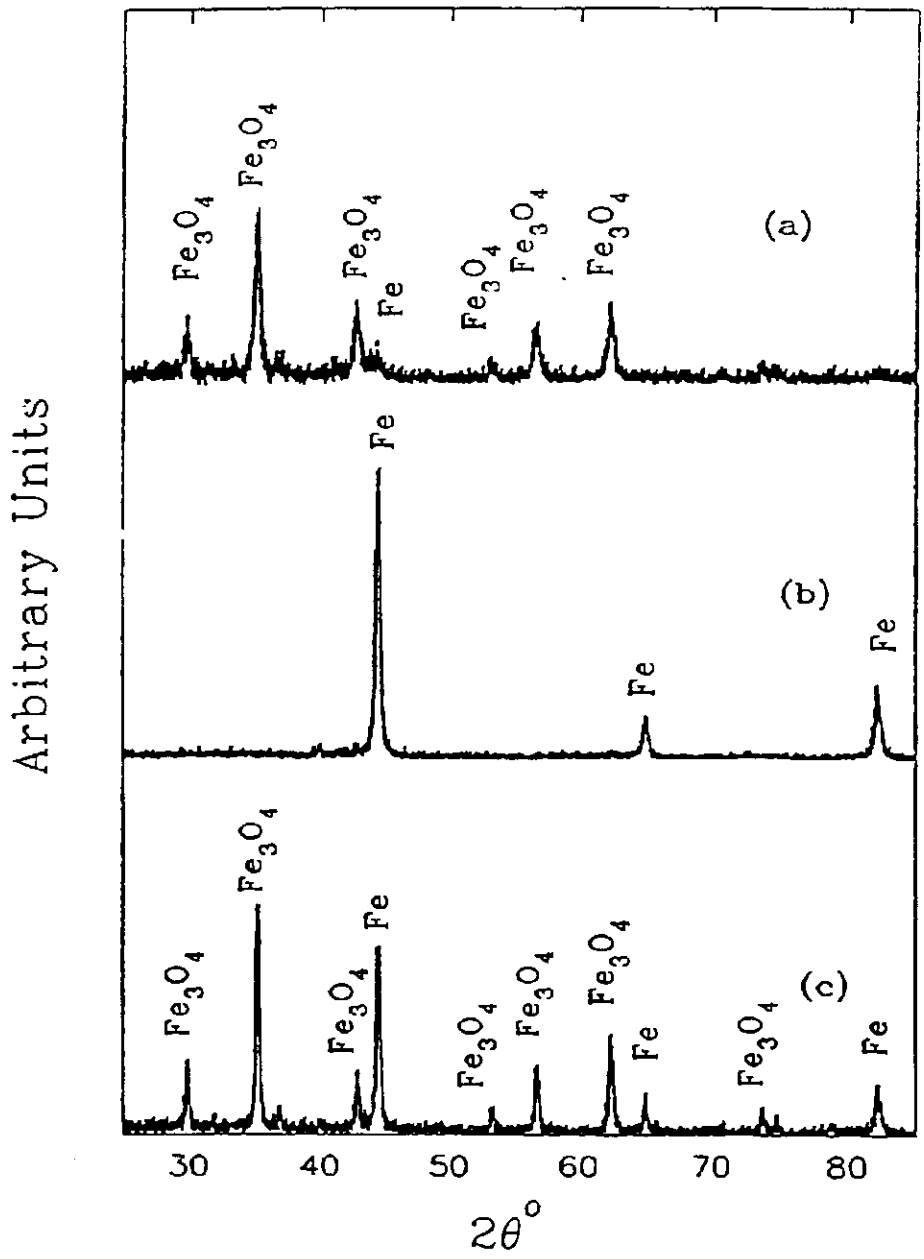

Figure III-1.2 XRD patterns of 100 Fe/0.3 Cu/0.8 K catalyst samples after pretreatment with H_2 at: a) 220°C for 1 h (flow rate = 3550 cc/min); b) 250°C for 2 h (flow rate = 3550 cc/min); c) 280°C for 8 h (flow rate = 85 cc/min).

Again, this can be attributed to the sintering/agglomeration of the particles on reduction.

The XRD pattern obtained after hydrogen reduction at 280°C for 8 h and at a flow rate of 85 cc/min showed the existence of Fe_3O_4 and Fe phases (see Figure III-1.2 c). It is important to note that in spite of higher reduction temperature and longer duration of reduction than in the previous cases, the reduction was incomplete. The flow rate used, however, was lower than in the previous two H_2 reduction procedures. It has been proposed earlier that water formed during reduction plays an important role in the determination of the iron phases formed (Dry, 1981; Anderson, 1984; Bukur et al., 1989a). At higher activation temperatures, water is released more rapidly and the partial pressure of water is higher than that occurring during reduction at lower temperatures. This, coupled with a low H_2 flow rate, results in high water partial pressure during reduction at 280°C. At these high partial pressures of water, partial reoxidation of the iron phases may occur. It is not clear whether mass transfer also plays an important role in such a reduction process. Low flow rate coupled with high reaction rate may result in relatively low mass transfer rates and, thus, in partial reduction of the catalyst. The particle size of metallic Fe estimated from the XRD slow scan was greater than that obtained after reduction at 250°C (33 vs. 24 nm). This may be due to the fact that higher water partial pressure enhances the rate of sintering of iron particles resulting in larger crystallite sizes.

When CO was used for pretreatment peaks at 2θ=39, 41, 43, 45, and 58° appeared (see Figure III-1.3a). These peaks were assigned to Hägg carbide (χ-Fe_5C_2) phase. This suggests that after 8 hours of pretreatment with CO at 280°C complete carburization of the oxide occurred. The particle sizes after pretreatment with CO could not be estimated due to overlapping signals of the Hägg carbide. The XRD patterns after pretreatment with syngas at 280°C for 8 h and 310°C for 6 h are illustrated in Figures III-1.3b and III-1.3c, respectively. The phases identified are

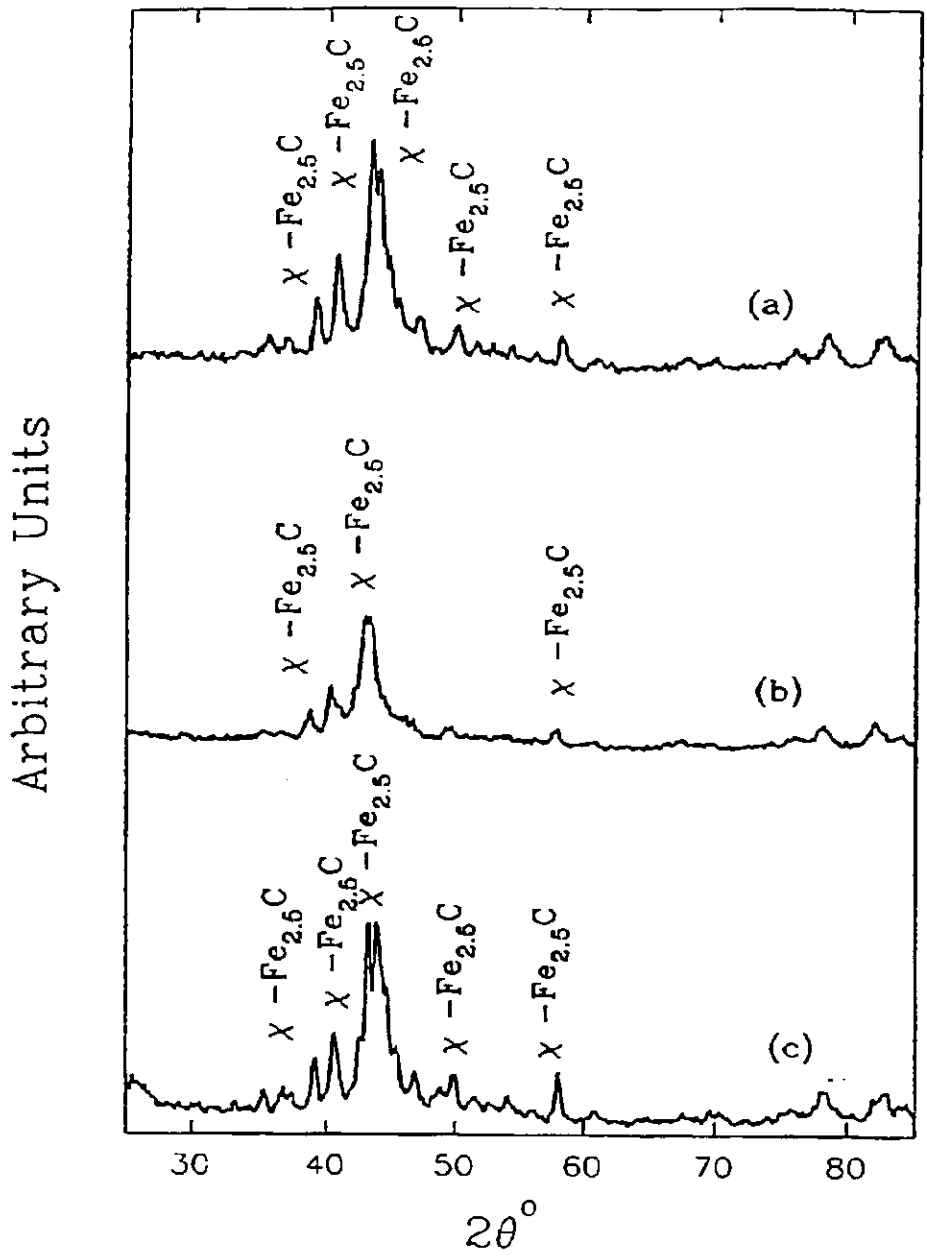

Figure III-1.3 XRD patterns of 100 Fe/0.3 Cu/0.8 K catalyst samples after pretreatment with CO or syngas: a) CO (85 cc/min) at 280 °C for 8h; b) syngas (H_2/CO=0.67, 85 cc/min) at 280 °C for 8h; c) syngas (H_2/CO=2.0, 1200 cc/min) at 310 °C for 6h.

summarized in Table III-1.1. It can be seen that even in the presence of H_2 no oxide/metallic iron phases could be detected. Hägg carbide was the only iron phase present after pretreatment with syngas. Since the presence of Fe/Fe_3O_4 depends on the relative rates of reduction (by H_2) followed by their carburization (by CO) it seems that the carburization of Fe or Fe_3O_4 is faster than the rate of H_2 reduction. In such a case no Fe/Fe_3O_4 would be expected after pretreatment with syngas. It is interesting to note that all the CO or syngas pretreatment procedures yield Hägg carbide regardless of the temperature, flow rate, or composition of the reducing gas. This suggests that the carburization of the iron phases is indeed rapid and may not be a strong function of the initial phase of iron. It has previously been reported that the use of promoters like Cu and K enhance the rate of carburization of precipitated iron catalysts (Vogler et al., 1984).

Used Catalyst Samples from Fixed Bed Reactor Tests

The XRD patterns of H_2 pretreated catalysts after FT synthesis in a fixed bed reactor are shown in Figure III-1.4. The used catalyst, pretreated with H_2 at 250°C (FB-0403), from the top part of the reactor consisted of a mixture of metallic iron and iron carbide phases (Figure III-1.4 a). In the bottom part, however, iron carbides (Fe_xC) were the most dominant phase detected along with weak Fe_3O_4 signals (Figure III-1.4b). Here, Fe_xC designates either a single iron carbide phase or a mixture of two iron carbide phases (χ or ε'). The precise identification of these two types of carbides is rather difficult when the signal intensities are low, and other compounds with overlapping peaks are present (Fe_3O_4, wax). Also, peak positions (2θ and the corresponding d-spacings) are sensitive to changes in height of a sample in the sample holder. In this report χ-carbide (Fe_5C_2) refers to the so called Hägg carbide, and its XRD pattern reported by Hoffer et al. (1949). Designation ε'- carbide ($Fe_{2.2}C$) is used to describe a pseudo-hexagonal iron carbide, which is also referred to as ε-Fe_2C carbide. Its XRD pattern was first reported by Barton and Gale (1964). The nature of

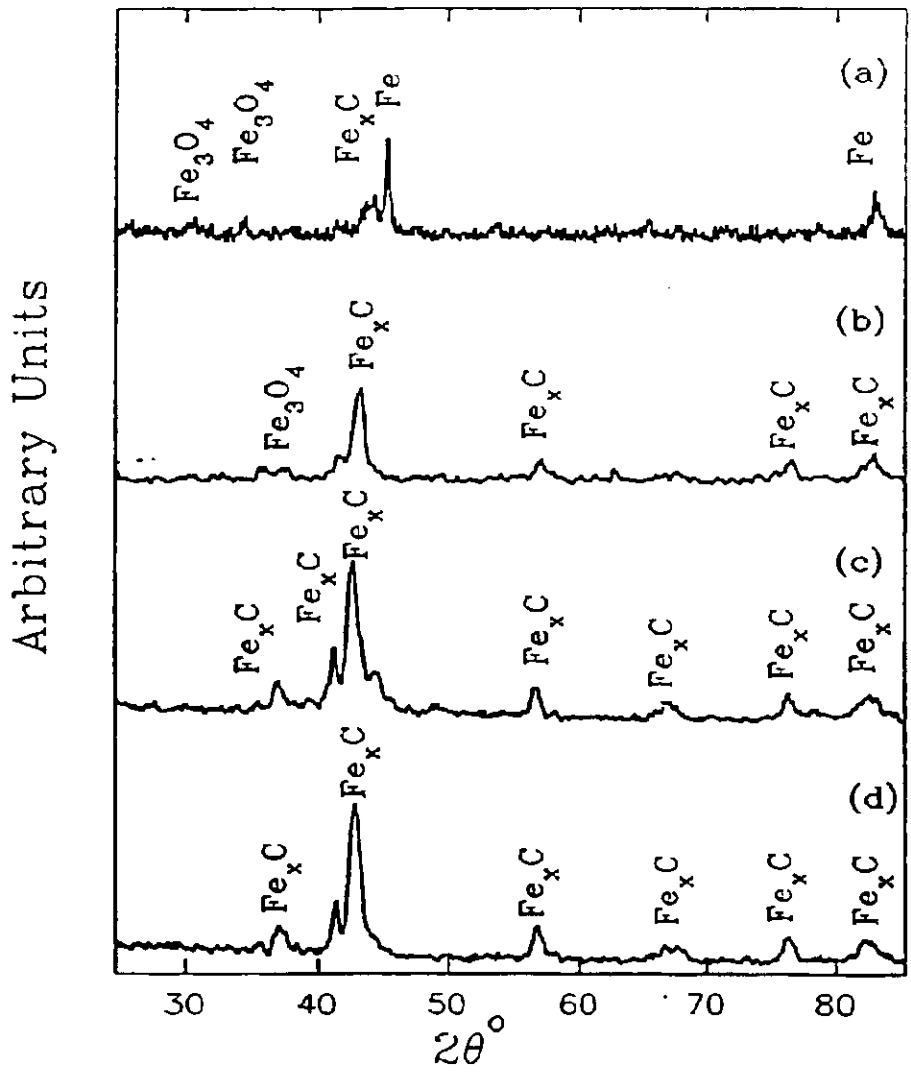

Figure III-1.4 XRD patterns of 100 Fe/0.3 Cu/0.8 K catalyst samples after FT synthesis and pretreatment with H_2: a) FB-0403 (top); b) FB-0403 (bottom); c) FB-3221 (top); d) FB-3221 (bottom) (see Table III-1.2 for the pretreatment conditions used).

iron carbide phases was determined by Mössbauer effect spectroscopy. The catalyst used in run FB-0403 was completely reduced to metallic iron (α-Fe) prior to FT synthesis, whereas in the presence of CO under FTS conditions Fe_xC was the dominant phase. This is consistent with the trend observed earlier when the catalyst was pretreated with syngas, and suggests that the rate of carburization of Fe and/or oxides is higher than that of reduction of oxides to metallic Fe. The presence of Fe_3O_4 in the used catalyst has been reported earlier in the literature (Dry, 1981; Anderson, 1984; Berry and Smith, 1989; Davis and Tungate, 1991). It has been suggested that water vapor formed during FTS may influence the phase changes occurring during FTS (Anderson, 1984). Water formed during FTS is responsible for the reoxidation of Fe/Fe_xC to Fe_3O_4. The particle size estimated from the slow scan for the top and bottom parts of the reactor is listed in Table III-1.2. The crystallite size of the used catalyst is similar to that of the reduced catalyst.

It should be noted that effective H_2/CO ratios are different in different parts of the reactor. In addition, due to water and CO_2 formed during FTS, H_2O/H_2 and CO_2/CO ratios are higher in the bottom part than in the top part of the reactor. This results in a reducing environment in the top part of the reactor, and an oxidizing environment in the bottom part of the reactor. Thus phases present in the top and bottom parts of the reactor may be different depending on the differences in gas composition in the reactor. Also, differences may exist in the relative amounts of these phases in the top and bottom parts of the reactor. However, XRD measurements cannot easily yield the quantitative results (i.e. relative amounts of iron phases in the sample). The similarities/differences in the relative amounts of iron phases estimated by Mössbauer effect spectroscopy are discussed later.

The used catalyst, pretreated with H_2 at 280°C, from top part of the reactor consisted of Fe_xC and Fe phases (Figure III-1.4c). As explained earlier, the particle size of the carbide(s) could not be obtained due to overlapping signals. Also, for this

Table III-1.2 Summary of XRD Results of 100 Fe/0.3 Cu/0.8 K Catalyst Samples after FT Synthesis - Fixed Bed Reactor Tests.

Run No.	Pretreatment Conditions; Time on Stream (TOS)	Phases Detected by XRD[a]	Average Particle Size Determined by XRD (nm)
FB-0403	H_2, 250°C, 2h; TOS=140h	Top: α-Fe, Fe_xC[c], Fe_3O_4	19 (α -Fe)[b]
		Bottom: Fe_xC, Fe_3O_4	23 (Fe_3O_4)[b]
FB-3221	H_2, 280°C, 8h; TOS=155h	Top: Fe_xC	--
		Bottom: Fe_xC	
FB-0021	CO, 280°C,8h; TOS=140h	Middle: Fe_3O_4, Fe_xC, $FeCO_3$	31 (Fe_3O_4)[b]
FB-0352	H_2/CO=0.67 280°C, 8h; TOS=150h	Top: Fe_xC	
		Bottom: Fe_3O_4, Fe_xC	33 (Fe_3O_4)[b]
FB-0942	H_2/CO=2, 310°C, 6h; TOS=142h	Top: Fe_xC	
		Bottom: $FeCO_3$	42 ($FeCO_3$)[b]

a: Phases are in decreasing order of relative intensities.
b: Indicates the phase used for particle size determination.
c: Fe_xC denotes iron carbide phase(s).

catalyst sample, the particle size of Fe could not be obtained due to weak Fe signals (Figure III-1.4c). In the bottom part of the reactor only Fe_xC phase was detected (Figure III-1.4d) indicating that the carburization was near complete in the bottom part of the reactor.

The XRD patterns of used catalysts pretreated with CO or syngas are shown in Figure III-1.5. The XRD pattern of the used catalyst, pretreated with CO, showed peaks

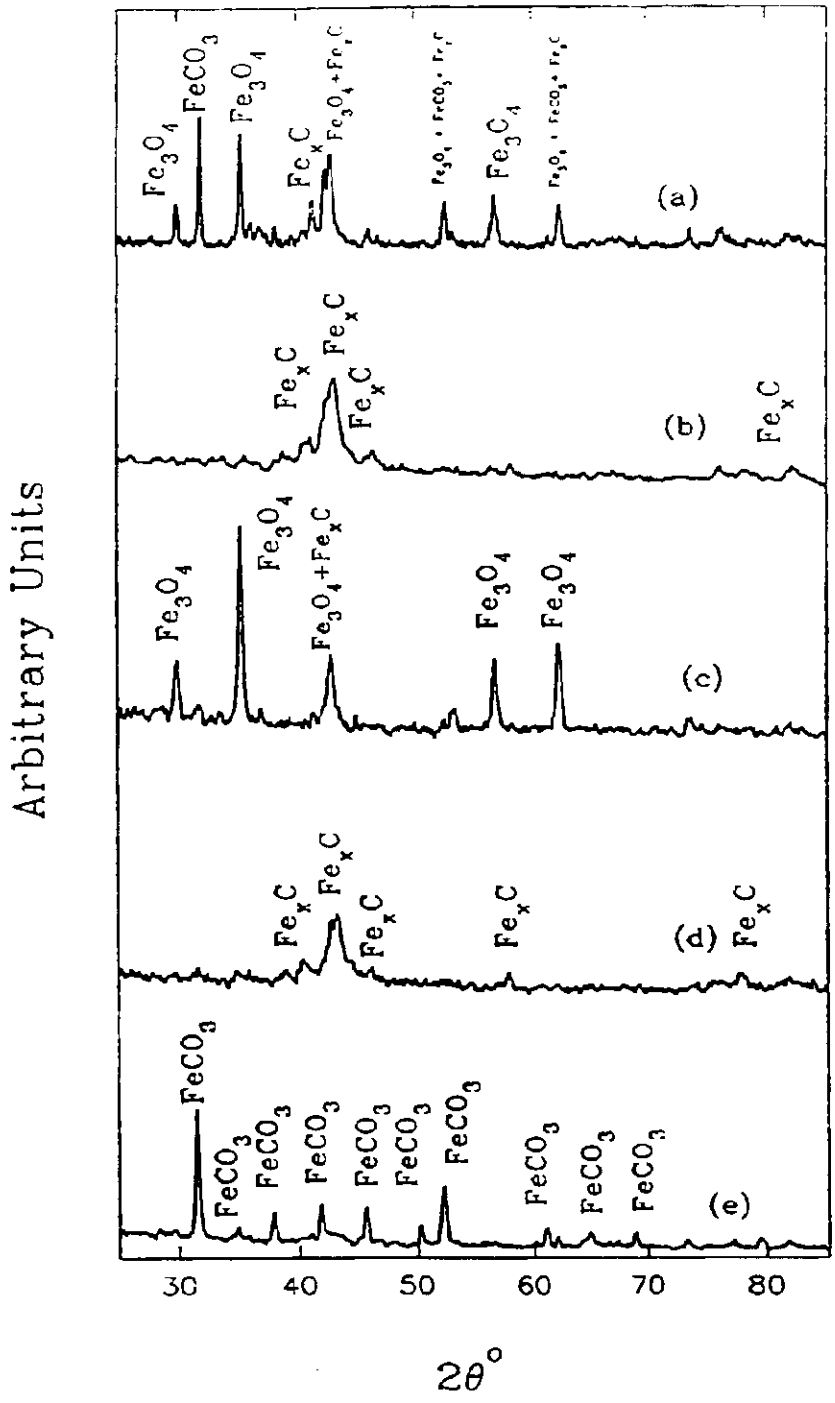

Figure III-1.5 XRD patterns of 100 Fe/0.3 Cu/0.8 K catalyst samples after FT synthesis and pretreatment with CO or syngas: a) FB-0021 (middle); b) FB-0352 (top); c) FB-0352 (bottom); d) FB-0942 (top); e) FB-0942 (bottom) (see Table III-1.2 for the pretreatment conditions used).

at 2θ = 32, 38.2, 52.5° which were assigned to $FeCO_3$ (siderite). In addition. Fe_xC and Fe_3O_4 phases were also detected. The particle size of the Fe_3O_4 phase estimated from the corresponding XRD slow scan is listed in Table III-1.2. The presence of siderite in the used precipitated iron catalyst was reported earlier (Anderson, 1984). It is possible that CO_2 formed by the water gas shift reaction plays a role in the formation of siderite. The reason why this phase is formed only in some cases is unclear at this time.

When pretreated with syngas (H_2/CO=0.7) at 280°C for 8 h, XRD pattern of the used catalyst sample from the top portion of the reactor showed the existence of Fe_xC phase (Figure III-1.5b), whereas in a sample from the bottom part of the reactor Fe_3O_4 could also be detected (Figure III-1.5c). The average particle size of Fe_3O_4 phase is about 33 nm. The XRD pattern of the used catalyst, pretreated with syngas at 310°C for 6 h, from the top part of the reactor showed the existence of Fe_xC phase (Figure III-1.5d). However, in the bottom part of the reactor only siderite ($FeCO_3$) could be detected (Figure III-1.5e). The presence of siderite was confirmed by the Mössbauer effect spectroscopy. The average particle size of the $FeCO_3$ phase is 42 nm, which is the largest crystallite size found in used catalyst samples (see Table III-1.2).

Used Catalyst from Slurry Reactor Tests

Used 100 Fe/0.3 Cu/0.8 K catalyst samples from slurry phase FT tests were also characterized by XRPD. In order to explain the similarities/differences in the activity/selectivity of the catalysts during FT tests as a function of time on stream, information on the phase changes with time is necessary. The catalyst samples withdrawn from a slurry reactor were separated from wax as described earlier and XRD measurements were made without exposure of samples to air.

Figure III-1.6 shows XRD patterns of the used 100 Fe/0.3 Cu/0.8 K catalyst samples from two slurry runs (SB-2262 and SA-0791) at various time on stream (TOS) values. In run SB-2262, the catalyst was pretreated with syngas (H_2/CO=0.7) at

280°C for 12 h, whereas in run SA-0791 the catalyst was pretreated with H_2 at 250°C for 2 h. The XRD pattern of the catalyst from run SB-2262 drawn prior to the FT synthesis (TOS=0 h) exhibited major peaks at 2θ=30.1, 35.4, 41, 43, 57, and 62.5°. Some minor peaks were also found above 2θ> 70° (Figure III-1.6a). As indicated earlier, the peaks at 30.1, 35.4, 43, 57, and 62.5° were assigned to Fe_3O_4 (magnetite) phase. The peaks at 41, 43 and peaks above 70° can be assigned to carbide phase(s) designated as Fe_xC. The exact assignment of these peaks to any single carbide phase is difficult since the peaks for most of the carbide phases are at similar positions. The closest match, however, was obtained for the Fe_2C (monoclinic) phase. The phases identified are summarized in Table III-1.3.

The XRD pattern of the catalyst drawn after 54 h on stream (T=250°C, SV=2 Nl/g-cat/h, P=1.5 MPa, H_2/CO=0.7) is shown in Figure III-1.6b. It can be seen that the peak at 35.4 and 62.5° have decreased considerably whereas the peak at 43° has increased with time. Since the carbide peaks and the magnetite peaks overlap at 2θ = 43 and 57°, the appearance/disappearance of the magnetite phases can be monitored by observing the peaks at 35.4 and 62.5°. Although the amounts of the phases cannot be quantitatively determined by XRD, the relative change in the intensities would at least qualitatively indicate changes in the phases with time on stream. Thus, it can be seen that the Fe_3O_4 phase decreased with time on stream whereas the Fe_xC phases seemed to have increased with time. This suggests that progressive carburization of iron oxide(s) occurred under FT conditions.

Figure III-1.6c shows the XRD pattern after 283 hours of reaction. There were two regeneration procedures carried out prior to this sampling; one after 162 h (H_2, 260°C, 4 h) and the other after 224 h (H_2, 280°C, 12 h). It can be seen from Figure III-1.6c that peaks at 35.4 and 62.5° disappeared completely while new peaks at 38, 39, 45, and 49° appeared indicating the formation of some new phase(s). Again, an unambiguous assignment of the new peaks to any particular phase was difficult.

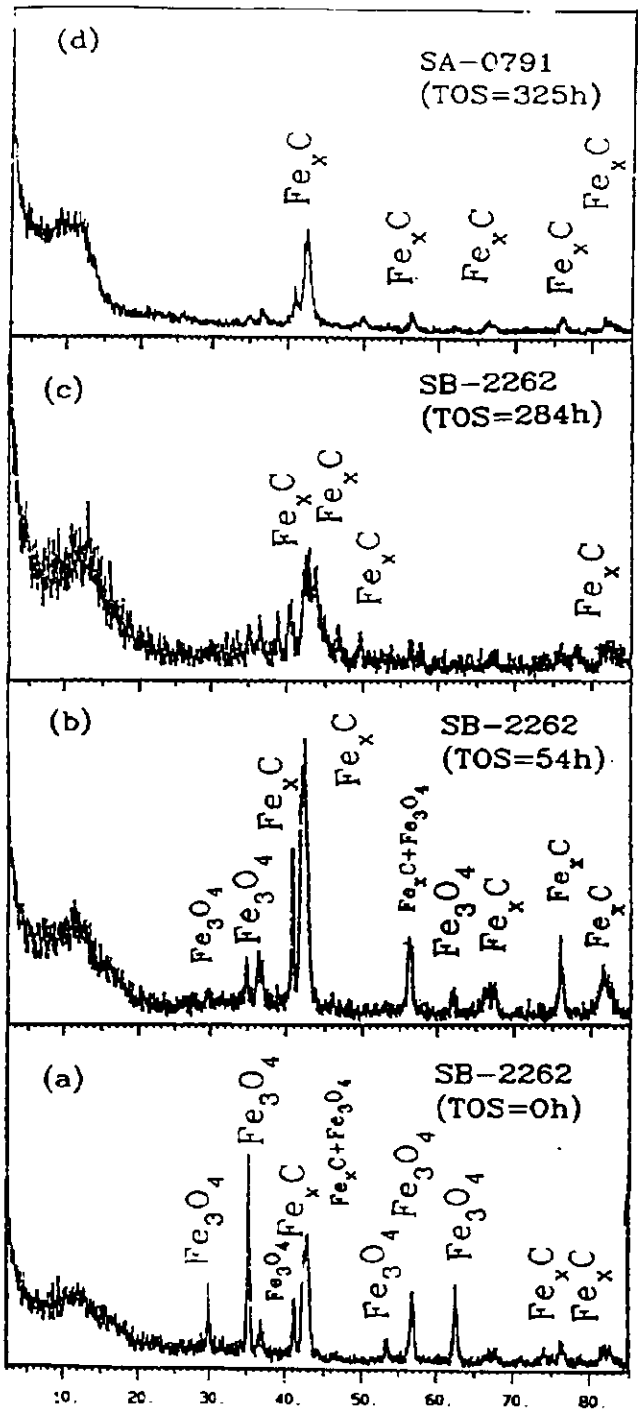

Figure III-1.6 XRD patterns of 100 Fe/0.3 Cu/0.8 K catalyst samples after FT synthesis in slurry reactor tests: a) SB-2262; TOS=0 h; b) SB-2262; TOS=54 h; c) SB-2262; TOS=284 h; d) SA-0791; TOS=325 h.

Table III-1.3 Phases Identified by XRD and MES in 100 Fe/0.3 Cu/0.8 K Catalyst after FT Synthesis - Slurry Phase Reactor Tests.

Run No.	Pretreatment Conditions	Time on Stream (hours)	Phases Identified by XRD	Phases Identified by MES[a]
SA-0791	H_2, 250°C, 2h	325	Fe_xC[c]	
SB-2262	H_2/CO=0.7, 280°C, 12h	0	Fe_3O_4, Fe_xC	ε'-$Fe_{2.2}C$ (54%), Fe_2O_3 (38%), Spm[b] (8%)
		54	Fe_xC, Fe_3O_4	ε'-$Fe_{2.2}C$ (86%), χ-Fe_5C_2 (7%), Fe_3O_4 (7%)
		284	Fe_xC	χ-Fe_5C_2 (93%), Spm (7%)

a: Numbers in paranthesis indicate the relative amount of the phases.

b: Superparamagnetic (spm) iron oxide/hydroxide.

c: Fe_xC denotes iron carbide phase(s).

However, some of these peaks can be assigned to χ-carbide. These phases are listed in Table III-1.3. Thus, despite the two regeneration processes with hydrogen, the catalyst sample at 283 h contained only iron carbide(s). Thus, the complete carburization of iron oxides occurred under FT conditions.

Figure III-1.6d shows the XRD pattern of the catalyst from run SA-0791 after 325 h on stream. At the end of the run (TOS=325 h), Fe_xC was the only component detected. Comparison of the bulk phases from runs SB-2262 and SA-0791 reveals

that although different pretreatment procedures were employed in these two tests, the carbide phases were the only phases detected after 280 h of FT synthesis. This means that complete carburization of the bulk iron oxides occurred during the course of the run regardless of the pretreatment procedure used.

III-1.2.3 Mössbauer Effect Spectroscopy (MES)

Although XRD is useful in determining the phases present in the catalyst after pretreatment and after FTS, the relative amounts of these phases cannot be easily quantified. The advantages of MES in determining the nature and the amounts of iron phases in the catalysts are well known (Amelse et al., 1978, Raupp and Delgass, 1979 a,b). In order to obtain a quantitative information on the bulk phases present in the reduced and used iron catalyst after pretreatment with H_2, CO, and syngas Mössbauer effect spectroscopy (MES) was used. The Mössbauer spectra were obtained and analyzed at the University of Kentucky (The Consortium for Fossil Fuel Liquefaction Science).

Reduced (Pretreated) Catalyst

Results of MES measurements are summarized in Table III-1.4. The Mössbauer spectrum of the catalyst sample, reduced with H_2 at 250°C for 2h, indicated the presence of metallic Fe only, which is consistent with the results from XRD analysis. Hydrogen reduction at 220°C for 1h resulted in formation of magnetite, and a small amount of superparamagnetic oxide/hydroxide phase. An upper limit to the particle size can be obtained from the occurrence of superparamagnetism. Kündig et al. (1966) have found that the critical diameter of Fe_2O_3 for superparamagnetic relaxation at room temperature is about 13.5 nm. In our case, some iron oxide particles are superparamagnetic indicating that the particle size is less than 13.5 nm. Low temperature measurements are needed to determine the exact nature of iron phases

Table III-1.4 Relative Amounts of Phases Identified by Mössbauer Effect Spectroscopy in Pretreated 100 Fe/0.3 Cu/0.8 K Catalyst Samples.

Run No.	Pretreatment Conditions	Spm[a] (%)	Magnetite (%)	χ-Carbide (%)	ε'-Carbide (%)	Fe-metal (%)
FA-2451	H_2, 220°C, 1h	11	81	—	8	—
FA-2491	H_2, 250°C, 2h	—	—	—	—	100
FA-2751	H_2, 280°C, 8h					
FA-2531	CO, 280°C, 8h	13	—	87	—	—
FA-2601	H_2/CO=0.67 280°C, 8h	16	—	84	—	—
FA-2581	H_2/CO=2, 310°C, 6h	5	—	95	—	—

a: Superparamagnetic (spm) iron oxide/hydroxide

exhibiting superparamagnetic properties. The presence of ε'-carbide in the reduced sample is attributed to the contamination of the sample with traces of another sample during sample preparation and handling.

The major phase in CO and syngas pretreated catalyst samples was χ-carbide (84-95%), the remainder being superparamagnetic oxide/hydroxide phase. This is in agreement with the results from XRD analysis.

Used Catalyst Samples From Fixed Bed Reactor Tests

Figure III-1.7a shows a typical Mössbauer spectrum obtained at 300 K of the used catalyst sample, pretreated with H_2 at 250°C, from the top part of the reactor (FB-0403). The spectral parameters (Isomer shift - IS; Hyperfine field - H, and Quadrupolar

split - QS) are typically obtained from such spectrum. The peak assignment is generally carried out by fitting such a spectrum to a known set of phases. For example, the spectrum shown in Figure III-1.7a could be fitted with three sets of sextets and a doublet (represented by a stick chart in Figure III-1.7a). The resultant values of H were 330 and 205 kGauss and can be assigned to Fe metal and Hägg carbide, respectively (Raupp and Delgass, 1979b). The amounts of phases identified are listed in Table III-1.5. The XRD pattern of this sample indicated the presence of Fe and Fe_xC phases which is in agreement with the MES results. However, iron oxide/hydroxide phase could not be detected by XRD either because of the low amount of this phase in the sample, or because of small particle size (less than 4 nm). Low temperature MES measurements are needed to determine the nature of superparamagnetic phase consisting of fine particles.

The relative amounts of iron phases in the catalyst sample, pretreated with H_2 at 250°C, from the bottom part of the reactor (FB-0403) are also listed in Table III-1.5. It can be seen that ε'-carbide (hexagonal close-packed) was the predominant phase in the bottom part of the reactor. The amount of χ-carbide, however, decreased from the top part of the reactor to the bottom part of the reactor from 64 to 7%, respectively. The phases identified are in agreement with the XRD results (Table III-1.2). It should be noted that MES results confirm the presence of Fe_3O_4 (magnetite) in the sample from the bottom part of the reactor.

The phases identified by MES for the catalyst sample, pretreated with H_2 at 280°C, from the top part of the reactor (FB-3221) are listed in Table III-1.5. Two carbide phases (χ-carbide and ε'-carbide) were predominant indicating that thecarbiding is near complete in the top part of the reactor. The used catalyst from the bottom part of the reactor also showed the existence of ε'-carbide and χ-carbide phases. The relative amount of ε'-carbide increased from 57% in the top part of the reactor to 95 % in the bottom part, whereas that of χ-carbide decreased from 36% in

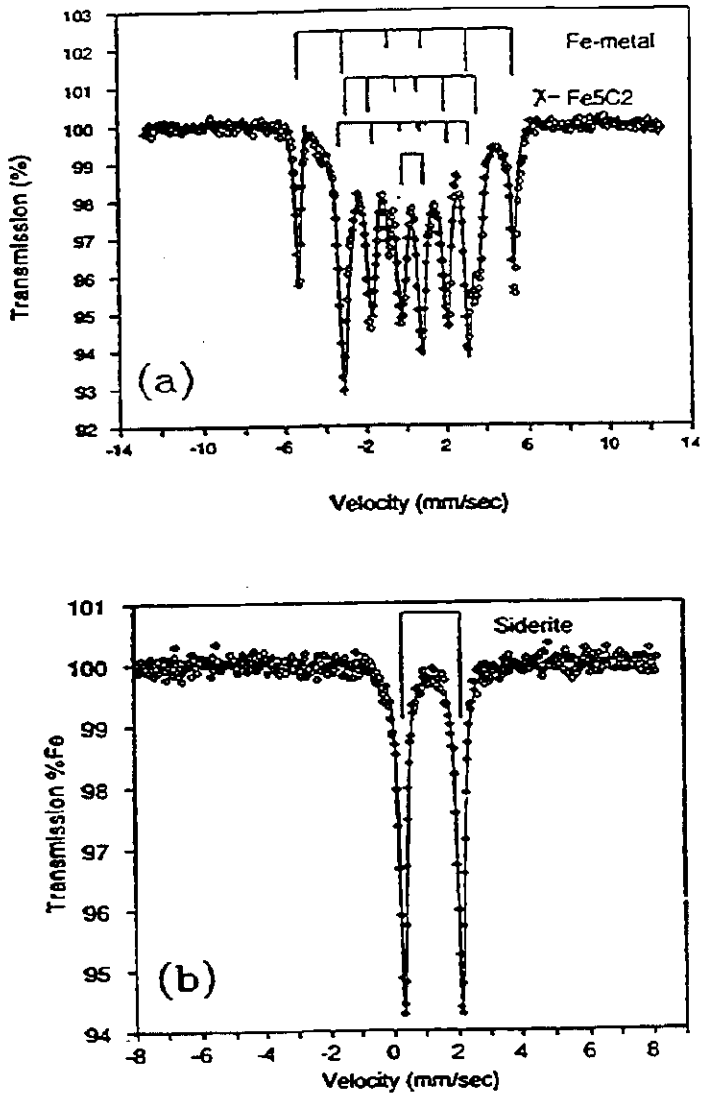

Figure III-1.7 Mössbauer spectra of 100 Fe/0.3 Cu/0.8 K catalyst samples after FT synthesis in a fixed bed reactor: a) FB-0403 (top); b) FB-0942 (bottom) (see Table III-1.2 for the pretreatment conditions used).

Table III-1.5 Relative Amounts of Phases Identified by Mössbauer Effect Spectroscopy in 100 Fe/0.3 Cu/0.8 K Catalyst Samples after FT Synthesis.

Run No.	Position	Pretreatment Conditions; TOS	Spm[a] (%)	Magnetite (%)	χ-Carbide (%)	ε'-Carbide (%)	Fe-Metal (%)	Siderite (%)
FB-0403	Top	H_2, 250°C, 2h; TOS=140h	13	—	64	—	23	—
FB-0403	Bottom		8	14	7	71	—	—
FB-3221	Top	H_2, 280°C, 8h; TOS=155h	7	—	36	57	—	—
FB-3221	Bottom		—	—	5	95	—	—
FB-0021	Middle	CO, 280°C, 8h; TOS=140h	2	50	—	43	—	5
FB-0352	Top	H_2/CO=0.67 280°C, 8h; TOS=150h	6	—	94	—	—	—
FB-0352	Bottom		9	59	—	32	—	—
FB-0942	Top	H_2/CO=2, 310°C, 6h; TOS=142h	35	—	65	—	—	—
FB-0942	Bottom		—	—	—	—	—	100

a: Superparamagnetic (spm) iron oxide/hydroxide

the top part to 5 % in the bottom part of the reactor. In general, the measurements are consistent with results obtained from XRD analysis.

In summary, the MES results for H_2 pretreated catalyst indicate significant carbiding under FTS conditions. The type of carbide formed, however, varies along the reactor. Raupp and Delgass (1979 b) found that the type of carbide formed was

dependent on the particle size of the iron phase. Larger iron particles tend to form χ-carbide, whereas smaller iron particles form the less stable ε'-carbides. Also, it is possible that the gas composition in the reactor influences the phases formed during FTS. As stated earlier, the reducing atmosphere exists at the top of the reactor, whereas the oxidizing atmosphere exists at the bottom of the reactor.

For the catalyst pretreated with CO at 280°C (FB-0021), Fe_3O_4, ε'-carbide, siderite, and superparamagnetic iron oxide/hydroxide phases were detected (see Table III-1.5). Several interesting observations can be noted from the MES results. Firstly, after CO pretreatment only the Hägg carbide was present in the catalyst as indicated by the XRD and MES measurements (Tables III-1.1 and III-1.4). However, in the used catalyst only the ε'-carbide phase was detected. Secondly, an iron carbonate (siderite) was identified by MES, which is in agreement with the XRD measurements. Finally, Fe_3O_4 is present in the used catalyst whereas none was detected initially. The reason for the formation of Fe_3O_4 was discussed earlier. However, the reason for the phase transformation from χ-carbide to ε'-carbide during FTS is not clear.

In the used catalyst, pretreated with syngas (H_2/CO=0.7) at 280°C (FB-0352), from the top part of the reactor, χ-carbide (94%) and superparamagnetic oxide (6%) were detected. The catalyst from the bottom part of the reactor consisted of Fe_3O_4, ε'-carbide, and superparamagnetic iron oxide/hydroxide phases (Table III-1.5). This is consistent with the phases identified by XRD. It can be seen that a significant amount of magnetite is observed in the used catalyst from the bottom part of the reactor for reasons explained earlier. Again, the ε'-carbide phase is found at the bottom part of the reactor, whereas the χ-carbide is found in the upper part of the reactor.

Iron phases in the used catalyst samples, pretreated with syngas (H_2/CO=2.0) at 310°C (FB-0942), from the top and bottom parts are listed in Table III-1.5. In the catalyst sample from the top part of the reactor, χ-carbide and oxide/hydroxide phases

were detected. The amount of superparamagnetic iron oxides in the catalyst was relatively large (about 35%). However, no iron oxide phases were detected by XRD measurements probably because of their fine particle size (less than 4 nm). The used catalyst from the bottom part of the reactor shows only $FeCO_3$ (siderite). Figure III-1.7b shows the MES pattern of siderite, which is characterized by a doublet with an isomer shift of 1.21 mm/s. The presence of siderite is consistent with the XRD pattern of the catalyst shown in Figure III-1.5.

Used Catalyst From Slurry Reactor Tests

The Mössbauer spectra of the used catalyst samples from slurry reactor tests were obtained as a function of time on stream. The relative amounts of phases identified by MES are listed in Table III-1.3. In the catalyst sample withdrawn prior to FT synthesis (Run SB-2262, syngas pretreatment at 280°C, for 12 h) the following phases were identified: ε'-carbide (54%), γ-Fe_2O_3 (38%), and superparamagnetic iron oxide (8%). The XRD pattern for this catalyst sample indicated the presence of Fe_3O_4 and Fe_xC phases (Table III-1.3). It is possible that magnetite phase in the pretreated sample was oxidized to γ-Fe_2O_3 due to exposure of the catalyst to air before and/or during MES measurements. The composition of catalyst sample withdrawn from the reactor after 54 h on stream (T=250°C, SV=2 Nl/g-cat/h, P=1.5 MPa, H_2/CO=0.7) is given in Table III-1.3. It can be seen that the relative amount of the carbide phases (ε' carbide + χ-carbide) increased from 54 % to 93 %, whereas the amount of oxide phases decreased. This shows that progressive carburization of the catalyst occurs under FTS conditions. The amounts of phases identified by MES after 283 h on stream are also shown in Table III-1.3. There were two regeneration procedures carried out prior to this sampling; one after 162 h (H_2, 260°C, 4 h) and the other one after 224 h (H_2, 280°C, 12 h). At 283 h on stream, the catalyst consisted of χ-carbide (93%) and superparamagnetic iron oxide (7%) phases. Thus, despite the two reduction procedures at 162 and 224 h on stream, χ-carbide was the most dominant phase at

283 h indicating that complete carburization of iron phases occurred under FT conditions. This is in agreement with the results from XRD analysis.

III-1.2.4 Isothermal Reduction Experiments

Isothermal reduction, using CO as the reductant, at 280°C for 8h was carried out by switching from He to CO at 280°C and monitoring the composition of the effluent gas by mass spectrometry as a function of time on stream. Figure III-1.8a shows the relative concentration profiles of reductant CO and product CO_2 (formed during reduction) up to 150 minutes. It can be seen that CO_2 profile shows a sharp peak at about 5 minutes followed by a broad maximum after about 40 minutes of reduction (Figure III-1.8a). This means that the rate of reduction of the catalyst is very rapid initially (up to 10 minutes). Similar behavior was observed earlier during isothermal reduction with CO of a 100 Fe/1 Cu/0.2 K catalyst at 300°C (Bukur et al., 1989b). This peak is probably due to the reduction of Fe_2O_3 to Fe_3O_4. The second broad peak may be due to the reduction of Fe_3O_4 to Fe and further carburization to iron carbides. The rate of reduction, as indicated by the formation of CO_2, gradually decreased after 150 minutes. However, a small amount of CO_2 was detected even after 8 hours of reduction.

The concentrations of CO and CO_2 were also obtained by gas chromatography at 12 minute intervals. Although data could not be acquired as rapidly with a gas chromatograph as with an on-line mass spectrometer, the CO_2 profile so obtained is in quaiitative agreement with the profile seen in Figure III-1.8a.

The amount of CO_2 formed during reduction up to about 8 hours was obtained from the CO_2 concentration profile shown in Figure III-1.8a. For this purpose, the data obtained by mass spectrometry were converted into absolute molar flow rates of CO_2 after proper calibration of the mass spectrometer using several known concentration values obtained by gas chromatography and the total flow effluent flow rate.

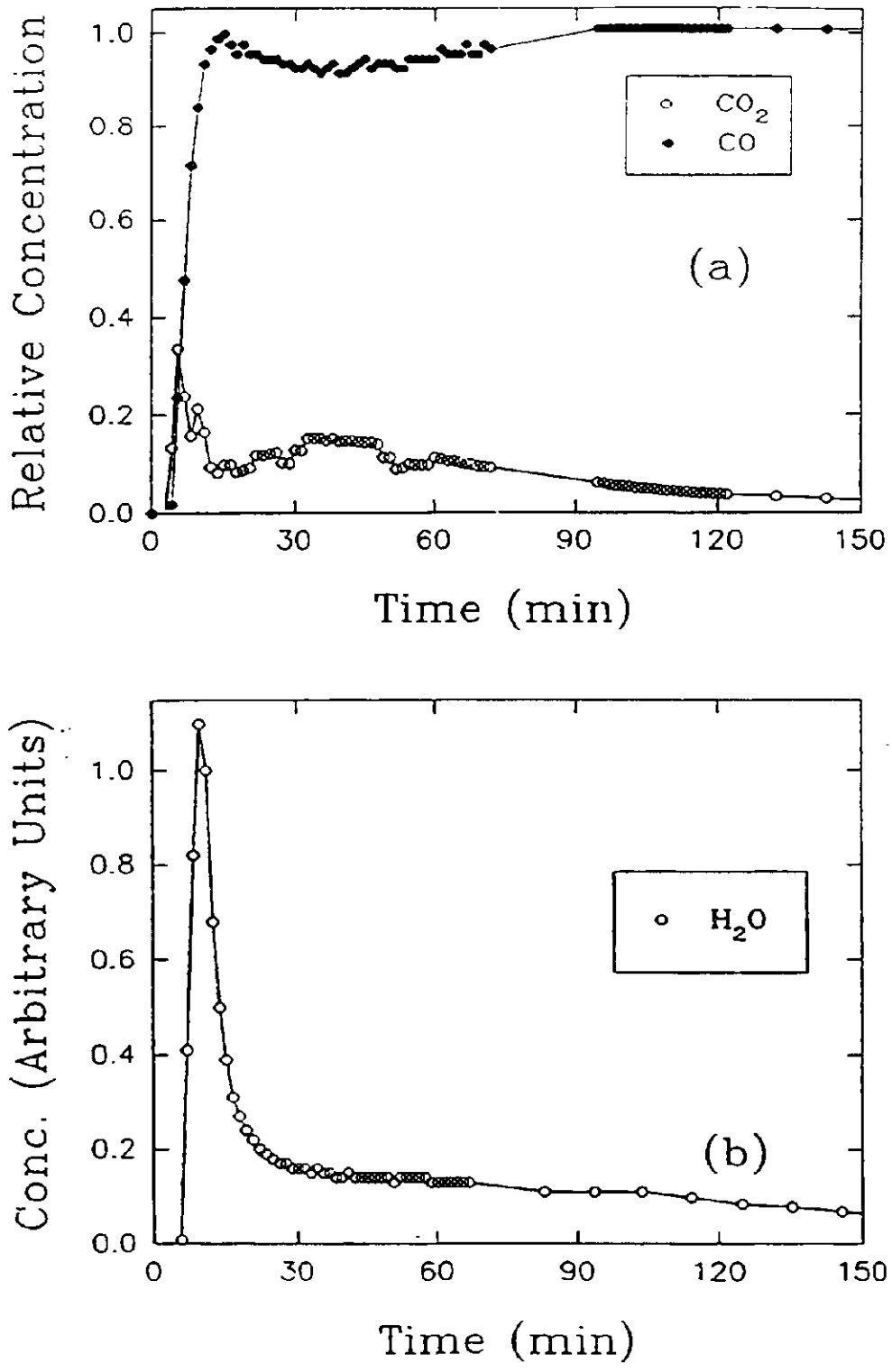

Figure III-1.8 Isothermal reduction profiles for 100 Fe/0.3 Cu/0.8 K catalyst at 280°C as a function of duration of reduction: a) CO reduction; b) H_2 reduction.

Integration of the CO_2 molar flow rate profile yielded the total amount of CO_2 formed up to 8 hours of reduction as 47 mmol/g of catalyst. It should be noted that the total amount of CO_2 that can be accounted for assuming complete reduction of the catalyst is 18.7 mmol/g. Whereas, the total amount of CO_2 that can be formed assuming complete carbiding of the catalyst (to $Fe_{2.2}C$) is 5.6 mmol/g. This means that the total amount of CO_2 formed far exceeds the amount of CO_2 that can be accounted for by both reduction as well as carburization. The excess CO_2 is presumably due to the formation of carbonaceous deposits on the catalyst.

Isothermal reduction profile obtained for H_2 reduction of the catalyst at 280°C for 8 hours, as seen by the formation of water, is illustrated in Figure III-1.8b. A sharp peak at about 10 minutes of reduction indicates rapid initial reduction. However, the rate of reduction decreases gradually after about 30 minutes. Similar reduction behavior was observed with 100 Fe/3 Cu/0.2 K catalyst during reduction with H_2 at 300°C (Bukur et al., 1989b). The sharp peak can attributed to the reduction of Fe_2O_3 to Fe_3O_4 whereas the slow reduction, i.e., after about 30 minutes, can be attributed to the reduction of Fe_3O_4 to metallic Fe. Quantitative information that could be obtained was limited due to lack of proper calibration methods for H_2O observed by mass spectrometry. However, the weight loss due to reduction was estimated at about 25 % of the total expected weight loss for reduction of Fe_2O_3 to Fe. Incomplete reduction of Fe_2O_3 after H_2 reduction under the above conditions was confirmed by XRD results, wherein Fe_3O_4 was detected (Table III-1.1). The incomplete reduction was also observed earlier (Bukur et al., 1989b) during the isothermal reduction of 100 Fe/3 Cu/0.2 K catalyst at 300°C.

III-1.2.5 BET Surface Area and Pore Size Distribution

The BET surface areas of as-prepared, calcined, and reduced samples are listed in Table III-1.6. The BET surface area was found to decrease after calcination

from 190 m^2/g to 130 m^2/g. This is probably caused by the collapse of pore structure due to removal of water of hydration from the highly porous $FeOOH/Fe_2O_3$ structure. Figure III-1.9 shows the pore size distribution of as-prepared and calcined samples. It can be seen that the distribution is fairly uniform with a maximum at approximately 6 nm. The average pore diameter calculated from measured values of the surface area and the pore volume are in good agreement with the pore diameter corresponding to the maximum in the pore size distribution curve (see Table III-1.6).

On pretreatment with H_2 at 220°C, the BET surface area decreased significantly (from 130 to 48 m^2/g). Likewise, the pore volume obtained by N_2 physiosorption also decreased significantly after reduction with H_2 (Table III-1.6). The decrease in the surface area after H_2 reductions at 250 and 280°C was even larger than that at 220°C.

It is known that as-prepared precipitated iron catalysts have high surface areas (Dry, 1981; Bukur et al., 1990b). A majority of the area is due to a highly porous iron network formed from small iron oxide particle agglomerates (about 15 nm; see Table III-1.6). The interparticle pores so formed are small in size and the network remains fairly stable even after low temperature calcination (300°C). On reduction, however, the porous structure collapses (in the absence of a suitable binder) resulting in sintering of iron particles (Dry, 1981). The fine pore structure disappears and the particles agglomerate to form larger clumps of particles. This increase in particle size translates into lower surface areas upon reduction. Similar behavior was observed by McCartney et al. (1950) and Hall et al. (1950). The decrease in the surface area due to increase in the particle size (as a result of sintering) can be calculated theoretically using a simple model which consists of uniform spherical particles. The surface area of such a model iron oxide system consisting of uniform spherical particles of size d can be expressed as: SA (per unit mass basis) = $6 / (\rho \times d)$; where ρ is the density of the particle.

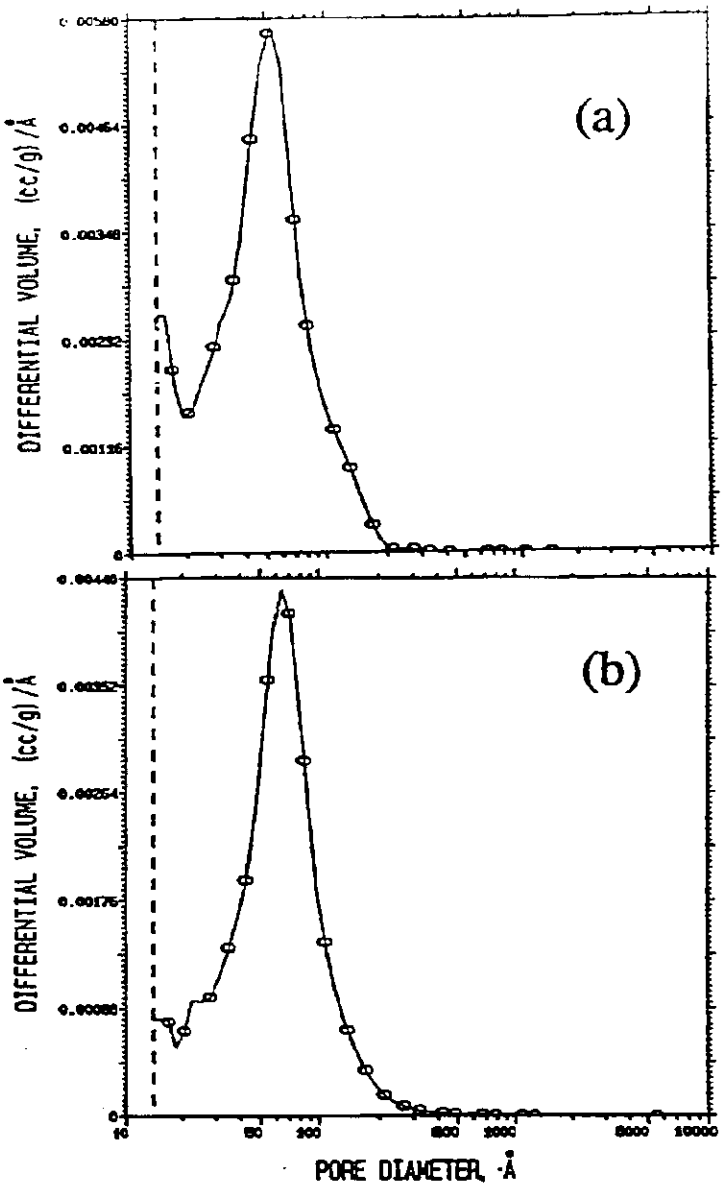

Figure III-1.9 Pore size distribution of 100 Fe/0.3 Cu/0.8 K catalyst:
a) as prepared; b) calcined in air at 300°C for 5h.

Table III-1.6 Summary of BET Results of Pretreated 100 Fe/0.3 Cu/0.8 K Catalyst Samples.

Run No.	Pretreatment Conditions	Surface Area (m^2/g)		Pore Volume (cc/g)		Pore Diameter (nm)	
		BET	Calc[a].	BET	Calc[b].	BET[c]	Calc[c]
As prepared	None	190	72 (Fe_2O_3)	0.33	0.496 (Fe_2O_3)	7	27.5
Calcined	Air, 300°C, 5h	130	82 (Fe_2O_3)	0.36	0.496 (Fe_2O_3)	11	24
FA-2451	H_2, 220°C, 1h	48	60 (Fe_3O_4)	0.25	0.502 (Fe_3O_4)	21	33
FA-2491	H_2, 250°C, 2h	21	32 (Fe)	0.20	0.330 (Fe)	38	41
FA-2751	H_2, 280°C, 8h	21	23 (Fe)	0.28	0.330 (Fe)	54	57
FA-2531	CO, 280°C, 8h	44	*	0.25	0.350 (Fe_xC)	23	*
FA-2501	H_2/CO=0.7, 280°C, 8h	34	*	0.30	0.350 (Fe_xC)	35	*
FA-2581	H_2/CO=2, 310°C, 6h	47	*	0.36	0.350 (Fe_xC)	31	*

a: Surface area = 6/(density x diameter); diameter from XRD measurements (Table III-1.1); phases used for density values are indicated in parenthesis.

b: Pore volume = 2.602/(density) ; phases used for density values are indicated in parenthesis.

c: Pore diameter=4 x pore volume/surface area; for BET pore diameters, measured BET surface areas and measured pore volumes were used, whereas for calculated pore diameters calculated values of surface area and pore volumes were used.

* The particle sizes could not be estimated using XRD because of overlapping signals.

The surface areas calculated using the above formula and the diameter of the particle determined by XRD are listed in Table III-1.6. The calculated surface area of the as-prepared and calcined samples is not in agreement with the measured surface area. However, the surface areas after H_2 reduction are in agreement with the measured BET surface areas. A possible reason for apparent disagreement between calculated and measured values of the surface area for the calcined and as-prepared catalysts is that in a real system the pore structure can be highly irregular (non-uniform particle sizes, interconnecting 3-dimensional pores; non spherical particles etc.).

This simple model can also be used to estimate the pore volume of the catalyst before and after reduction. Assuming particles of size d in a cubic closed packed (ccp) geometry (analogous to face centered cubic crystal structure) the pore volume per unit mass, V_p, is given by $V_p=2.602/\rho$. The pore volume depends on the density of the particle only and is independent of the particle size. It should be noted that the phase change on reduction leads to the formation of iron which is more dense than the corresponding oxides. The calculated pore volumes are listed in Table III-1.6. It can be seen that the calculated pore volumes are in fair agreement with the observed pore volumes considering the simplicity of the model involved.

Figure III-1.10 shows the pore size distribution after pretreatment with H_2. Although the pore size distribution is fairly uniform, i.e. with a single maximum (unimodal), the pore size corresponding to the maximum is considerably higher than that for the calcined catalyst. In fact, the position of maximum shifted to higher values with increase in the reduction temperature (from 15 nm at 220°C to 46 nm at 280°C; see Figure III-1.10). The average pore diameter calculated from the pore volume and the surface area is also listed in Table III-1.6, and is in reasonable agreement with that corresponding to the maximum of the pore size distribution curves. The average pore diameter was also estimated from the calculated values of surface areas and pore volumes (using the model described above). Although the calculated pore diameters

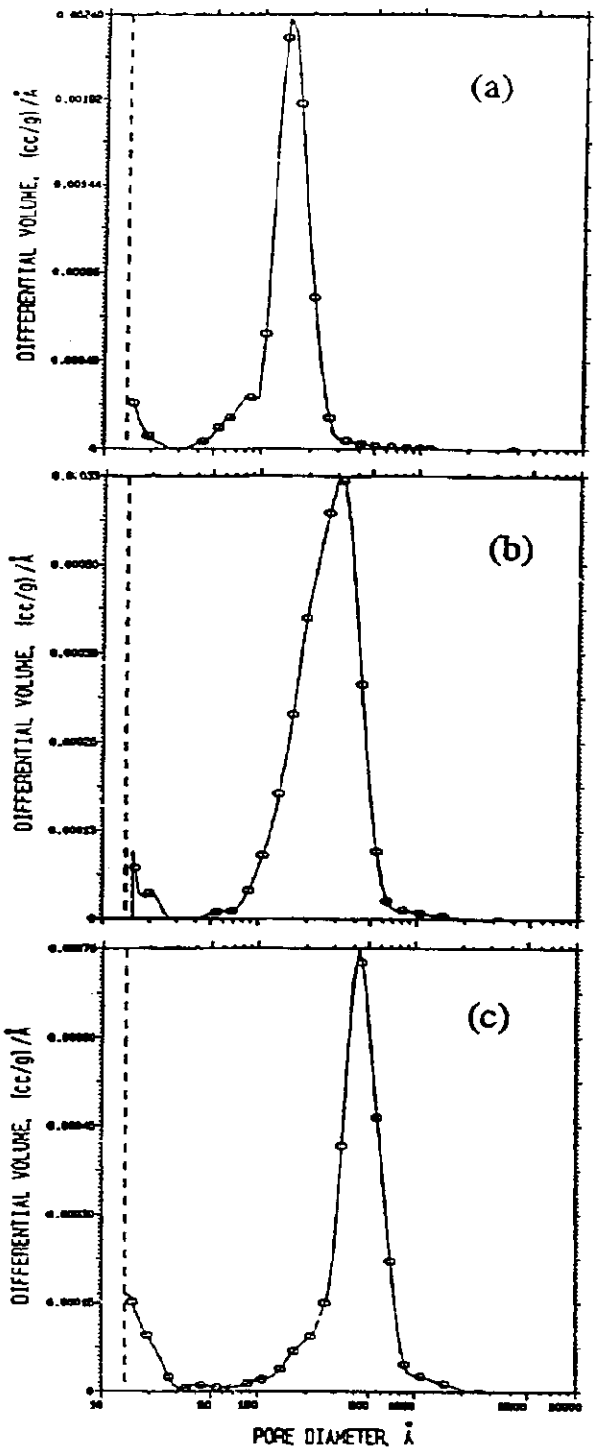

Figure III-1.10 Pore size distribution of 100 Fe/0.3 Cu/0.8 K catalyst after pretreatment with H_2 at: a) 220°C for 1 h (flow rate = 3550 cc/min); b) 250°C for 2 h (flow rate = 3550 cc/min); c) 28°C for 8 h (flow rate = 85 cc/min).

are over estimated for the calcined and as-prepared catalyst samples, the pore diameters after reduction are in agreement with the average pore diameter calculated from observed values of surface area and pore volume.

The surface area after pretreatment with CO or syngas also decreased significantly (see Table III-1.6). This may be attributed to particle sintering and collapse of the porous iron network as explained earlier. The surface areas could not be estimated from the model described earlier since the particle size was not determined by XRD. The pore volume decreased after pretreatment with CO. However, no significant change in the pore volume was observed when the catalyst was pretreated with syngas. In order to explain this, it is necessary to examine the pore size distribution of the catalyst.

Figure III-1.11 shows the pore size distribution (PSD) of the catalyst after pretreatments with CO and syngas. The pore diameter corresponding to the maximum in the PSD increased from 6 nm for the calcined catalyst to 13 nm after CO pretreatment (Figure III-1.11a). However, upon pretreatment with syngas the pore size distribution became increasingly bimodal as seen from a small shoulder in Figure III-1.11b, and from two distinct peaks (4 nm and 45 nm) in Figure III-1.11c. This suggests that on reduction with syngas smaller pores are also created, in addition to the formation of larger pores. The higher pore volume observed after syngas pretreatment is due to the formation of smaller pores. XRD analysis indicated the formation of carbide on reduction with syngas. It is possible that the carbide particle agglomerates have smaller pores whereas the large pore originate from the agglomerates of the oxide and/or bulk Fe particles. Also, it has been postulated earlier (Davis and Tungate, 1991) that a carbon overlayer is formed on pretreatment with CO or syngas. This overlayer is known to be porous and may posses fine pore structure. These small pores are probably responsible for higher pore volume after reduction with syngas.

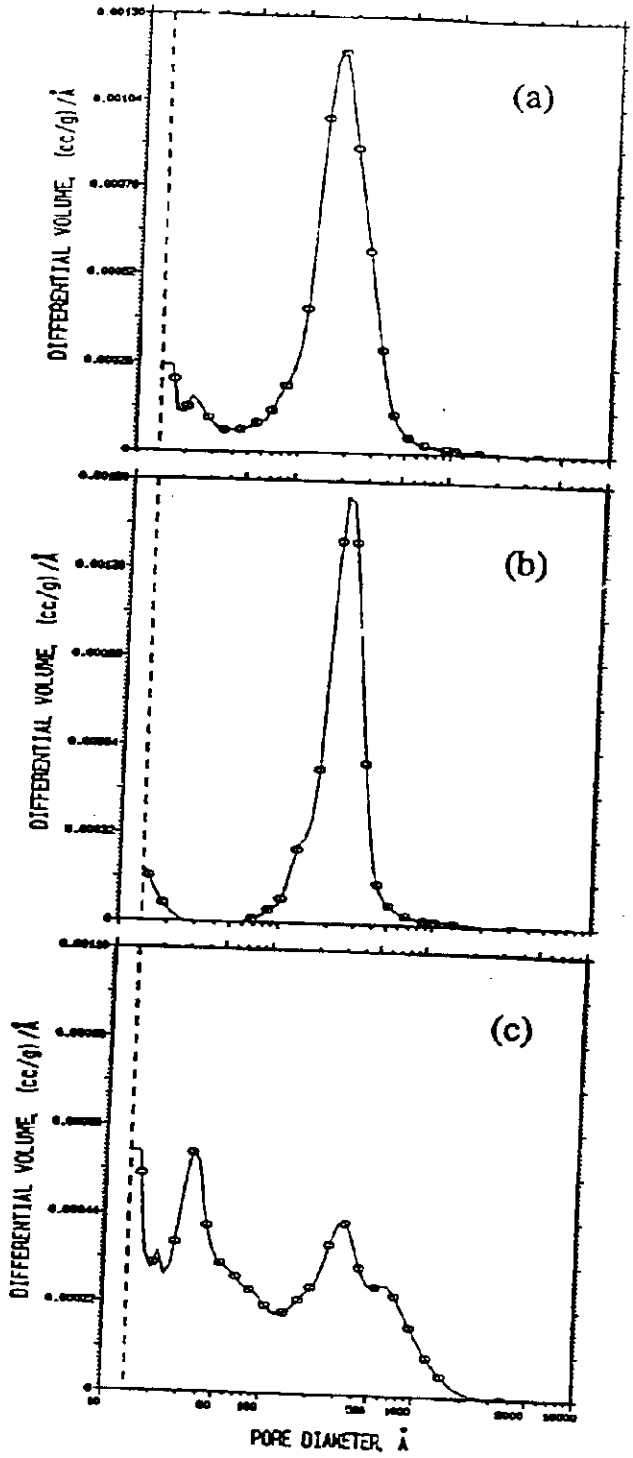

Figure III-1.11 Pore size distribution of 100 Fe/0.3 Cu/0.8 K catalyst after pretreatment with CO or syngas: a) CO (85 cc/min) at 280 °C for 8h; b) syngas (H_2/CO=0.67, 85 cc/min) at 280 °C for 8h; c) syngas (H_2/CO=2.0, 1200 cc/min) at 310 °C for 6h.

The BET surface area and the pore size distribution of the used catalyst samples were not obtained, since the catalyst was mixed with glass beads to maintain isothermal conditions during FTS and complete separation of catalyst particles from glass beads is difficult. Also, the used catalysts are covered with wax and possibly carbonaceous deposits, both of which would need to be removed before BET measurements.

III-1.2.6 Transmission Electron Microscopy

Figure III-1.12 shows the TEM micrographs of the calcined catalyst under two different magnifications. It can be seen that the particle morphology is essentially spherical. The particle size is approximately 26 nm. The micrographs of the reduced (pretreated) 100 Fe/0.3 Cu/0.8 K catalyst samples are shown in Figures III-1.13 and III-1.14. The particle size ranges obtained by TEM are summarized in Table III-1.1. After reduction with H_2, the particles exhibited a broader size range (Figure III-1.13). It should be noted that the large particles observed in these micrographs may in fact be aggregates of smaller particles. Generally, an average particle size can be determined from the electron micrographs only after careful statistical procedure and multiple sampling. In this case a precise estimation of average particle size was not obtained due to a broad distribution of particle sizes observed in these micrographs. In general, however, the particle size seems to have increased after reduction with H_2. In particular, after pretreatment with H_2 at 250°C, the particle size has increased significantly. Particles as large as 64 nm could be observed (Figure III-1.13b). The morphology, however, still remained essentially spherical. After pretreatment with H_2 at 280°C a similar increase in particle size was observed. This is consistent with the XRD results wherein a similar increase in the particle size was observed. As stated earlier, the increase in the particle size after H_2 reduction is probably due to the

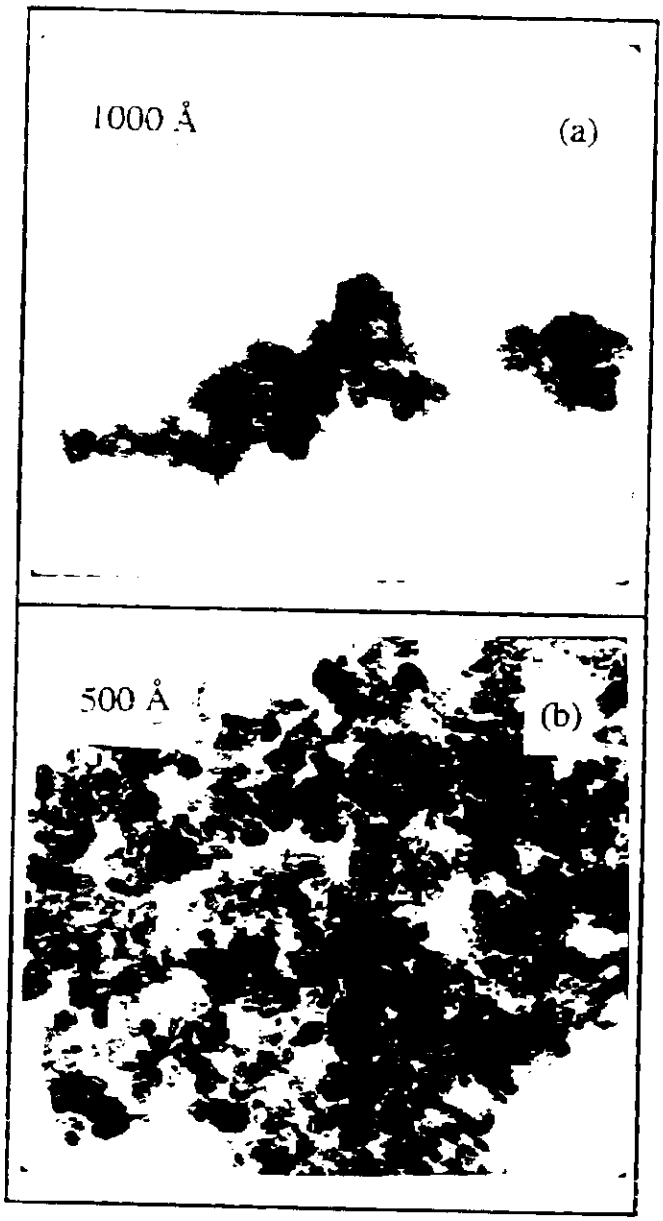

Figure III-1.12 TEM micrographs of calcined 100 Fe/0.3 Cu/0.8 K catalyst at different magnifications: a) 108,000 X; b) 140,000 X.

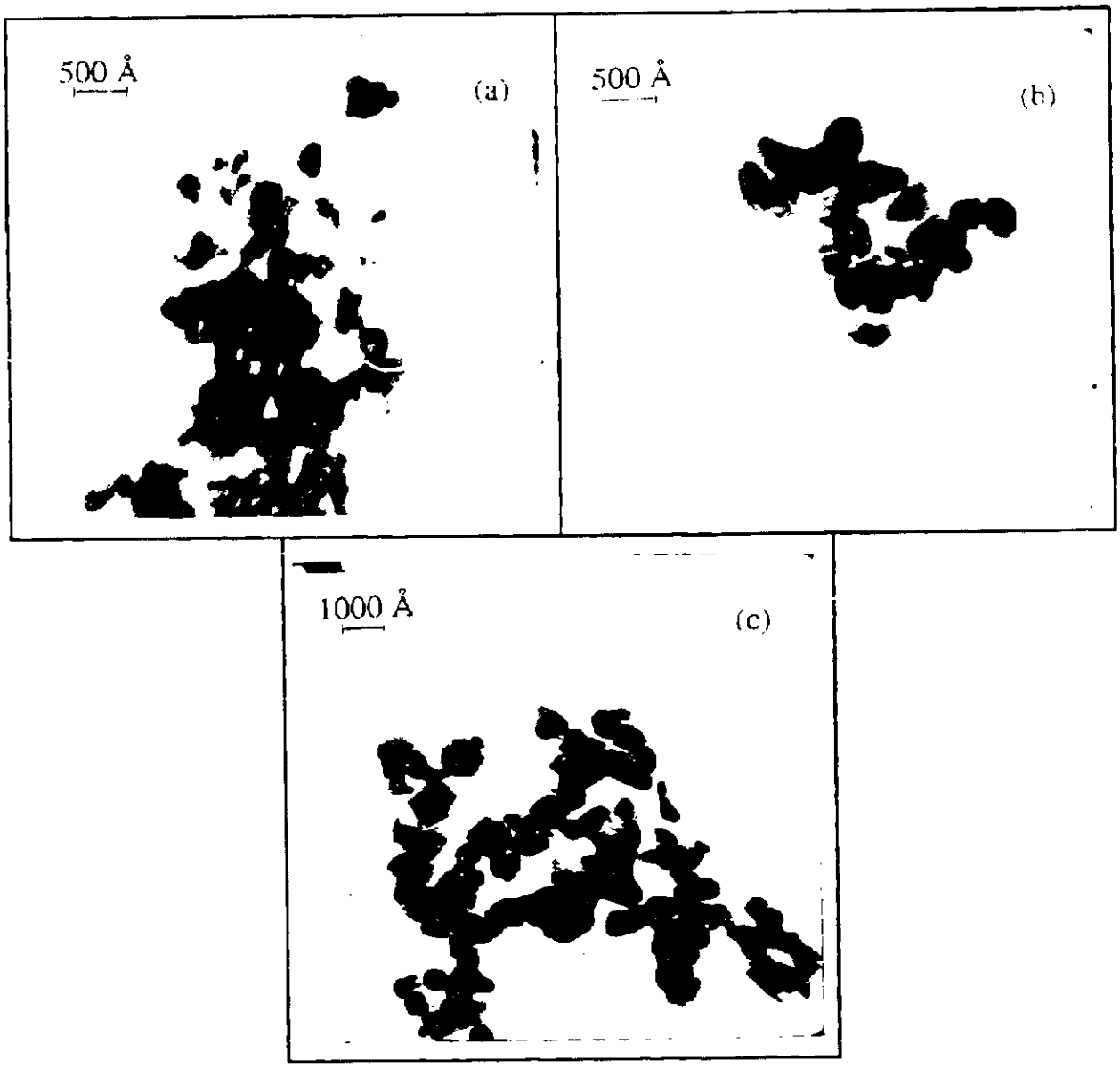

Figure III-1.13 TEM micrographs of 100 Fe/0.3 Cu/0.8 K catalyst samples after pretreatments with H_2 at: a) 220 °C for 8 h (flow rate = 3550 cc/min); b) 250 °C for 2 h (flow rate = 3550 cc/min); c) 280°C for 8 h (flow rate = 85 cc/min).

collapse of the highly porous Fe_2O_3 network. This behavior is also consistent with the observed decrease in the surface area on reduction.

Figure III-1.14 shows TEM micrographs after pretreatment with CO and syngas. The estimated particle sizes are listed in Table III-1.1. After CO or syngas pretreatment, the TEM micrographs indicate the presence of aggregates of small particles (10 nm) as well as those of large particles (>25 nm). The morphology of the catalyst remained largely spherical after CO or syngas pretreatment.

TEM micrograph of the used catalyst sample, reduced with H_2 at 250°C, is shown in Figure III-1.15. Both large (> 80 nm) and small (3-10 nm) particles were detected in this catalyst sample. Although some large particles may be aggregates of smaller particles, individual particles with sizes greater than 50 nm can be clearly distinguished. It is interesting to note that small particles are present after the FT synthesis reaction, even though large Fe or Fe_3O_4 particles were observed after H_2 reduction. The smaller particles were essentially spherical. However, the larger particles were either plate like (hexagonal) or needle shaped.

A comparison of the particle size determined by XRD and by TEM indicates that XRD underestimates the average particle size. Similar observations were made wherein the particles sizes (even single crystals) determined by XRD were smaller than those determined by TEM (Butt, 1990). This was attributed to the presence of faults (imperfections) in these particles. Imperfections cause the particle to diffract more or less like two (or many) smaller particles. Also, care should be taken when interpreting TEM data. The large particles may in fact be aggregates of smaller particles. The presence of carbonaceous deposits may also mask the original particle size. There have been hypotheses that a carbon overlayer (or filamentous carbon) is generally formed during FTS (Tungate and Davis, 1991; Vogt et al., 1987). Although this overlayer is believed to be porous, the particle size estimated from TEM may be overestimated. Such an overlayer can be seen in Figure III-1.15.

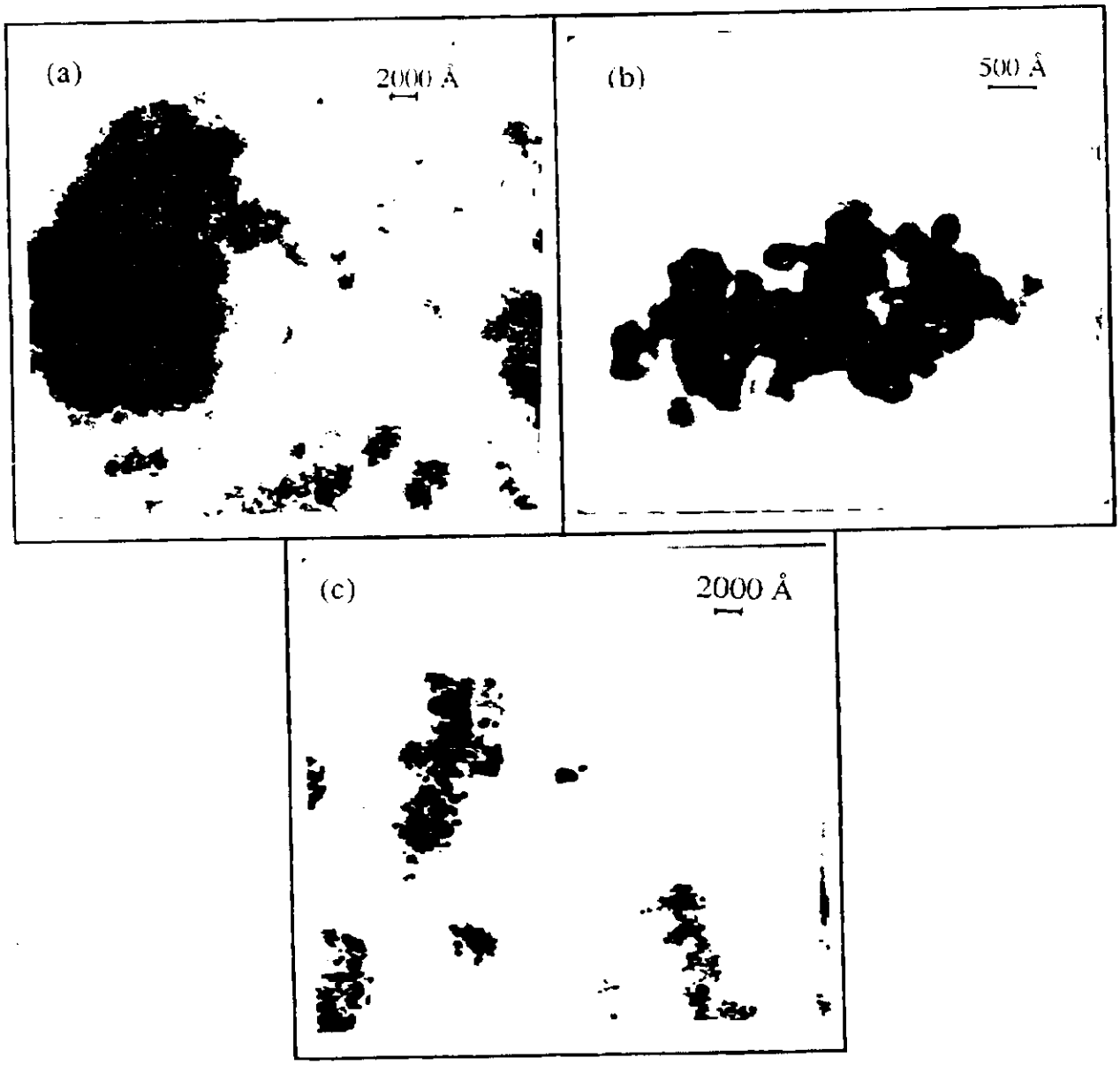

Figure III-1.14 TEM micrographs of 100 Fe/0.3 Cu/0.8 K catalyst samples after pretreatments with CO or syngas: a) CO (85 cc/min) at 280 °C for 8h; b) syngas (H_2+CO=0.67, 85 cc/min) at 280 °C for 8h; c) syngas (H_2+CO=2.0, 1,200 cc/min) at 310°C for 6h.

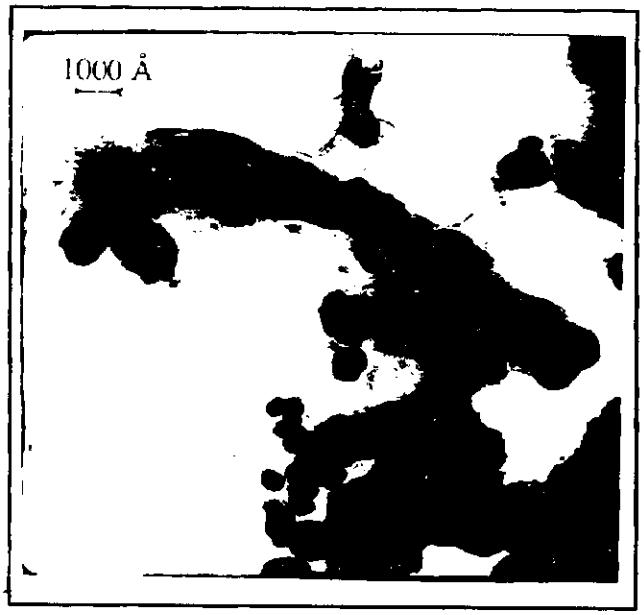

Figure III-1.15 TEM micrograph of 100 Fe/0.3 Cu/0.8 K catalyst after FT synthesis in the fixed bed reactor Run FB-0403.

III-1.3 Summary

The unsupported, doubly promoted precipitated iron catalyst with nominal composition 100 Fe/0.3 Cu/0.8 K was characterized before and after different pretreatments, and after Fischer-Tropsch synthesis in a fixed bed reactor at 250°C, 1.48 MPa (200 psig), 2 Nl/g-cat/h, H_2/CO = 0.67 for 140 - 200 h.

The BET surface area of the catalyst decreased from 190 m^2/g to 130 m^2/g after calcination in air at 300°C for 5 hours, and further to 21-47 m^2/g after pretreatments in hydrogen, carbon monoxide or syngas. The pore volume decreased upon pretreatments in H_2 or CO, but remained unchanged after syngas pretreatment. The pore size distribution of as-prepared and pretreated catalyst was essentially monomodal, and shifted to larger pore diameters after H_2 or CO pretreatments. However, the syngas pretreated catalyst had a bimodal pore size distribution with maxima at 4 and 45 nm. Transmission electron micrographs of samples before and after different pretreatments reveal that particles are largely spherical. An increase in particle size was observed after H_2 reductions both by TEM and XRD analysis. The particle size increased with reduction temperature (e.g. 19 nm after H_2 reduction at 220°C, and 33 nm after reduction at 280°C).

X-ray diffraction (XRD) and Mössbauer effect spectroscopy (MES) were used to identify bulk iron phases in pretreated and used (after FT synthesis) catalyst samples. Calcined catalyst is in the form of α-Fe_2O_3 (~ 16 nm in diameter), which is converted to either metallic iron (α-Fe) or a mixture of α-Fe and Fe_3O_4 (magnetite) after H_2 reductions. During FT synthesis the α-Fe is carburized to iron carbides (χ- Fe_5C_2 or ε' - $Fe_{2.2}C$) or oxidized to magnetite. The gas environment is predominantly reducing at the top of the reactor (since the syngas is introduced at the top), and more oxidizing at the bottom of the reactor due to formation of water and carbon dioxide. Thus, the catalyst samples from the top part of the reactor contain relatively more iron carbides

or metallic iron, whereas magnetite is found preferentially in samples from the bottom part of the reactor. Also, relative amounts of χ- Fe_5C_2 carbide are greater in the top part of the reactor than in the bottom part, whereas the opposite trend is observed for ε' - $Fe_{2.2}C$ carbide.

After CO or syngas pretreatments, the χ- Fe_5C_2 carbide is the most dominant phase. During FT synthesis this carbide is partially or completely converted to ε' - $Fe_{2.2}C$ carbide, Fe_3O_4, and/or $FeCO_3$ (siderite). Again it was found that the iron carbides are dominant in samples from the top part of the reactor (reducing atmosphere), whereas Fe_3O_4 or $FeCO_3$ are dominant iron phases in samples from the bottom part.

Temporal release of reduction products (water or carbon dioxide) was monitored continuously during H_2 and CO pretreatments by gas chromatography and mass spectroscopy. It was found that the reduction is very rapid initially (first 5 to 10 minutes), and then continues at a much lower rate. The reduction products were detected in the effluent gas after 8 hours of reduction at 280°C. This has been interpreted as a two step reduction process. The first (fast) step is the reduction of Fe_2O_3 to Fe_3O_4, which is followed by reduction of Fe_3O_4 to either metallic iron (H_2 reduction) or to an iron carbide (CO pretreatment). The second step is a slow one, and the reduction is not complete (H_2 reduction). The amount of CO_2 released during the CO pretreatment was greater than the stoichiometric amount needed for complete oxygen removal and complete carburization of iron in the catalyst. It is assumed that this is due to formation of carbonaceous deposits by Boudouard reaction.

III-1.4 References

Amelse, J. A.; Butt, J. B.; Schwartz, L. J. Carburization of Supported Iron Synthesis Catalysts. *J. Phys. Chem.*, **1978**, *82*, 558-563.

Anderson, R. B. Catalysts for the Fischer-Tropsch Syntheis In *Catalysis*; Emmett, P. H. Ed.; Van Nostrand-Reinhold: New York, 1956; Vol. IV, pp. 29-255.

Anderson, R. B. *The Fischer-Tropsch Synthesis*; Academic Press: Orlando, FL, 1984.

Barton, G. H. and Gale, B. The Structure of a Pseudo-Hexagonal Iron Carbide. *Acta Cryst.*, **1964**, *17*, 1460-1462.

Berry, F.J., and Smith, M.R. Mössbauer Investigation of Iron Containing Catalyst Prepared at Low Temperatures and Active Carbon for CO Hydrogenation. *J. Chem. Soc. Faraday Trans.*, I, **1989**, *85*, 467-474.

Blanchard, F.; Reymond, J. P.; Pommier, B.; Teichner, S. J. On the Mechanism of the Fischer-Tropsch Synthesis Involving Unreduced Iron Catalyst. *J. Mol. Catal.* **1982**, *17*, 171-181.

Bukur, D.B., Lang, X., Rossin, J.A., Zimmerman, W.H., Rosynek, M.P., Yeh, and E.B., Chiuping L. Activation Studies with a Promoted Precipitated Iron Fischer-Tropsch Catalyst. *Ind. Eng. Chem. Res.* **1989a**, *28*, 1130-1140.

Bukur, D.B., Mukesh, D., Patel, S.A., Rosynek, M.P., Zimmerman, W.H. Development and Process Evaluation of Improved Fischer-Tropsch Slurry Catalysts. Final Report to Air Products and Chemicals, Inc. under DOE Contract No. DE-AC22-85PC8011, 1989b: Texas A & M University, College Station, TX.

Bukur, D.B., Lang, X., Mukesh, D., Zimmerman, W.H., Rosynek, M.P., and Chiuping L. Binder/Support Effects on the Activity and Selectivity of Iron Catalysts in the Fischer-Tropsch Synthesis. *Ind. Eng. Chem. Res.* **1990b**, *29*, 1588-1599.

Butt, J.B. Carbide Phases on Iron-Based Fischer-Tropsch Synhtesis Catalysts - Part I: Characterization Studies. *Catalysis Letters*, **1990**, *7*, 61-82.

Butt, J. B. Carbide Phases on Iron-Based Fischer-Tropsch Synthesis Catalysts; Part II: Some Reaction Studies. *Catal. Letters* **1990**, *7*, 83-106.

Davis, B.H., and Tungate, F.L. Preparation of Precipitated Iron Fischer-Tropsch Catalyst. In DOE Contractors Review Meeting Proc., Pittsburgh PA, 1991, pp 275-289.

Dictor, R.; Bell, A. T. Fischer-Tropsch Synthesis over Reduced and Unreduced Iron Oxide catalyst. *J. Catal.* **1986**, *97*, 121-136.

Dry, M. E. The Fischer-Tropsch Synthesis. In *Catalysis - Science and Technology*; Anderson, J. R.; Boudart, M., Eds.; Springer - Verlag: New York, 1981; Vol. I, pp160-255.

Dwyer, D. J.; Somorjai, G. A. Hydrogenation of CO and CO_2 over Iron Foils: Correlation of Rate, Product Distribution and Surface Composition. J. *Catal.*. **1978**, *52*, 291-301.

Hall, K.W., Tarn, W.H., and Anderson, R.B. Studies of the Fischer-Tropsch Synthesis. Part VII. Surface Area and Pore Volume Studies of Iron Catalysts. *J. Am. Chem. Soc.* **1950**, *72*, 5436-5452.

Hofer, L. J. E., Cohn, E. M., Peeebles, W. C. The Modifications of the Carbide, Fe_2C; Their Properties and Identification. *J. Am. Chem. Soc.* **1949**, *71*, 189-195.

Kuivila, C. S.; Stair, P. C.; Butt, J. B. Compositional Aspects of Iron Fischer-Tropsch Catalysts: An XPS/Reaction Study. *J. Catal.* **1989**, *118*, 299-311.

Kündig, W., Bommel, H., Constabaris, G., Lindquist, R.H. Some Properties of Supported Small a-Fe_2O_3 Particles Determined with Mössbauer Effect. *Phys. Rev.* **1966**, *142*, 327 -342.

Matsumoto, H.; Bennett, C. O. The Transient Method Applied to the Methanation and Fischer-Tropsch Reaction over a Fused Iron Catalyst. *J. Catal* . **1978**, *53*, 331-344.

McCartney, J.T., Selegman, B., Hall, K.W., Anderson, R.B. An Electron-Microscopic Study of Metal Oxides and Metal Oxides Catalysts. *J. Phys. Chem.*, **1950**, *54*, 505-512.

Niemantsverdriet, J. W.; van der Kraan, A. M. On the Time-Dependent Behavior of Iron Catalyst in Fischer-Tropsch Synthesis. *J. Catal*. **1981**, *72*, 385-388.

Raupp, G.B., and Delgass, W.N. Mössbauer Investigation of Supported Fe and FeNi Catalysts. Part I: Effect of Pretreatment on Particle Size. *J. Catal.*, **1979a**, *58*, 337-347.

Raupp, G.B., and Delgass, W.N. Mössbauer Investigation of Supported Fe and FeNi Catalysts. Part II: Carbides Formed by Fischer-Tropsch Synthesis. *J. Catal.*, **1979b**, *58*, 348-360.

Reymond, J. P.; Meriadeau, P.; Teichner, S. J. Changes in the Surface Structure of an Iron Catalyst of Reduced or Unreduced Fe_2O_3 during the Reaction of Carbon Monoxide and Hydrogen. *J. Catal.* **1982**, *75*, 39-48.

Satterfield, C. N.; Hanlon, R. T.; Tung, S. E.; Zou, Z.; Papaefthymiou, G. C. Initial Behavior of a Reduced Fused-Magnetite Catalyst in the Fischer-Tropsch Synthesis. *Ind. Eng. Chem. Prod. Res. Dev.* **1986**, *25*, 401-407.

Soled, S.; Iglesia, E.; Fiato, R. A. Activity and Selectivity Control in Iron Catalyzed Fischer-Tropsch Synthesis. *Catal. Letters* **1990**, *7*, 271-280.

Vogler, G.L., Jiang, X.-Z., Dumesic, J.A., Madon, R.J. The Use of N_2O as a Surface Probe of Iron Catalyst for Fischer-Tropsch Synthesis. *J. Catal.*, **1984**, *89*, 116-129.

Vogt, E.T.C., van Dillen, A.J., and Geus, J.W. Prevention of Growth of Filamentory Carbon in Supported Iron and Nickel Catalysts. In Catalyst Deactivation, Delmon, B., and Froment G.F., Eds.; Elsevier, Amsterdam, 1987, pp 221-233.